Reproductive Biology and Endocrinology

Research

Origin of germ cells and formation of new primary follicles in adult human ovaries

Antonin Bukovsky*[1,2], Michael R Caudle[1,2], Marta Svetlikova[1] and Nirmala B Upadhyaya[2]

Address: [1]Laboratory of Development, Differentiation and Cancer, The University of Tennessee Graduate School of Medicine, Knoxville, Tennessee 37920, USA and [2]Department of Obstetrics and Gynecology, The University of Tennessee Graduate School of Medicine, Knoxville, Tennessee 37920, USA

Email: Antonin Bukovsky* - buko@utk.edu; Michael R Caudle - MCaudle@mc.utmck.edu; Marta Svetlikova - marta.svetlikova@centrum.cz; Nirmala B Upadhyaya - nbupadha@mc.utmck.edu

* Corresponding author

Published: 28 April 2004

Reproductive Biology and Endocrinology 2004, **2**:20

Received: 03 March 2004
Accepted: 28 April 2004

This article is available from: http://www.rbej.com/content/2/1/20

Abstract

Recent reports indicate that functional mouse oocytes and sperm can be derived in vitro from somatic cell lines. We hypothesize that in adult human ovaries, mesenchymal cells in the tunica albuginea (TA) are bipotent progenitors with a commitment for both primitive granulosa and germ cells. We investigated ovaries of twelve adult women (mean age 32.8 ± 4.1 SD, range 27–38 years) by single, double, and triple color immunohistochemistry. We show that cytokeratin (CK)+ mesenchymal cells in ovarian TA differentiate into surface epithelium (SE) cells by a mesenchymal-epithelial transition. Segments of SE directly associated with ovarian cortex are overgrown by TA, forming solid epithelial cords, which fragment into small (20 micron) epithelial nests descending into the lower ovarian cortex, before assembling with zona pellucida (ZP)+ oocytes. Germ cells can originate from SE cells which cover the TA. Small (10 micron) germ-like cells showing PS1 meiotically expressed oocyte carbohydrate protein are derived from SE cells via asymmetric division. They show nuclear MAPK immunoexpression, subsequently divide symmetrically, and enter adjacent cortical vessels. During vascular transport, the putative germ cells increase to oocyte size, and are picked-up by epithelial nests associated with the vessels. During follicle formation, extensions of granulosa cells enter the oocyte cytoplasm, forming a single paranuclear CK+ Balbiani body supplying all the mitochondria of the oocyte. In the ovarian medulla, occasional vessels show an accumulation of ZP+ oocytes (25–30 microns) or their remnants, suggesting that some oocytes degenerate. In contrast to males, adult human female gonads do not preserve germline type stem cells. This study expands our previous observations on the formation of germ cells in adult human ovaries. Differentiation of primitive granulosa and germ cells from the bipotent mesenchymal cell precursors of TA in adult human ovaries represents a most sophisticated adaptive mechanism created during the evolution of female reproduction. Our data indicate that the pool of primary follicles in adult human ovaries does not represent a static but a dynamic population of differentiating and regressing structures. An essential mission of such follicular turnover might be elimination of spontaneous or environmentally induced genetic alterations of oocytes in resting primary follicles.

Background

The possible formation of new primary follicles in adult human ovaries is a controversial issue. In order to give the readers relevant information on prior observations and current views, we are providing additional information on this subject.

Follicular nomenclature

In this study, we use the term primary for ≤ 50 μm diameter follicles (resting, primordial, intermediary and primary follicle types), and secondary for >50 and ≤ 100 μm (growing) follicles.

Origin of germ cells

The origin of oocytes (and primary follicles) in ovaries of adult mammalian females has been a matter of dispute since the proposal by Waldeyer in 1870 that germ cells arise from the proliferation of somatic coelomic (germinal or surface) epithelium of the presumptive gonad [1]. A contrary view was Weissmann's theory of the continuity of the germ plasm [2]. This theory assumes that during the earliest stages of embryonic development, before embryonic cells become committed along specific pathways, a set of germ cells is set aside, which are destined to give rise to the gametes. During the 1960's and early 1970's, this latter view was accepted for all animals, including mammals [3,4].

Utilization of newer techniques has shown that the Weissmann's theory may fit invertebrates (*C. Elegans and Drosophila*) and some lower vertebrates (zebrafish and frogs), but not mice, and possibly mammals in general [5]. Studies of mouse embryos, in which genetically marked cells were introduced at the 4- and 8-cell stage blastomere, have shown that such cells can either become germ cells or somatic cells [6]. This suggests that no specific germ cell commitment exists prior to implantation. During the postimplantation period, mouse germ cells are not identifiable before ~7 days after fertilization [7]. The germ cells differentiate from somatic lineage [8]. It has also been shown that cellular differentiation of grafted embryonic cells does not depend on where the grafts were taken, but where they have been placed [9]. Additional studies suggest an important role in the development of germ cells for Bone Morphogenetic Protein 4 (BMP4), a member of TGFβ superfamily, as null BMP4 mouse embryos failed to develop primordial germ cells [10].

More recently, oogenesis has been demonstrated in cultured mouse embryonic stem cells. Such oogonia entered meiosis, recruited adjacent cells to form follicle-like structures, and later developed into the blastocysts [11]. Cultured mouse embryonic stem cells have also been reported to differentiate into haploid male gametes capable of fertilizing eggs and develop into blastocysts [12]. Presumptive germline stem cells have been recently reported in ovaries of adult mice [13], resembling earlier observations of dividing germ cells in ovaries of adult prosimian primates [14-18].

Altogether, these studies indicate that somatic cells have the potential to develop into germ cells, and some mammalian species posses mitotically active germ cells in adult ovaries. Nevertheless, the paradigm that all primary follicles in adult mammalian females were formed during the fetal period of life is still supported by a sizable number of scientists, primarily because of the lack of direct evidence on formation of new primary follicles in adult mammalian ovaries [18]. It also remains unclear whether mitotically active germ cells in adult prosimians and presumptive germline stem cells in mice persist from the fetal period of life or differentiate *de novo* from some type of progenitor cells, if the number of dividing germ cells determines the number of new primary follicles, what the source of granulosa cells for newly formed follicles might be, and if a preservation of germ cells in these two species is an exception or the rule for other mammals, and human females in particular. In this report we propose that in adult human ovaries mesenchymal cells in the tunica albuginea (TA) are bipotent progenitors with a commitment for both primitive granulosa and germ cells.

Tunica albuginea, surface epithelium, and derived epithelial structures in human ovarian cortex

The human TA is a thick fibrous subepithelial layer of loose connective-tissue cells. It does not begin to form until the end of intrauterine life [19] or several months after the birth [20]. Even then it is not a true membrane, but merely a collection of loose connective-tissue cells [20]. In contrast to the ovarian surface epithelium (SE), supposedly the source of a variety of ovarian tumors, the TA has not been well studied.

The ovarian cortex is usually covered by a layer of irregularly shaped special epithelial-like mesothelial cells [21], commonly referred to as the ovarian "germinal", superficial, or surface epithelium. This layer is attached to the basal lamina continuous with the subjacent TA by means of collagenous fibrils. Except in the ovaries of newborn animals, mitoses are essentially absent in ovarian SE [22]. In functional human ovaries the SE is found in certain areas only, but in women with anovulatory cycles, or patients with polycystic or sclerotic ovaries, the ovarian surface is completely covered with SE [23]. This is despite similar handling during surgical retrieval, suggested by Gillett [24] to cause ovarian denudation.

In scanning electron microscopy and submicroscopic studies of ovarian SE during ovulatory cycles, it has been reported that the ovarian surface is frequently evaginated

into a series of villous-like projections or papillae, which may vary widely in the number, size, and distribution (reviewed in [21]). The SE also invaginates into the ovarian cortex throughout the entire organ. This is true in all mammalian species, including humans. Cortical invaginations appear as small elongated clefts, subsurface channel-like crypts, and solid cords of epithelial cells. Crypts are hollow, tubular invaginations lined by cells possessing the same general features as SE cells. However, the cord cells are very similar to some of the granulosa cells. In some areas of the ovary, cords fragment and appear as small 'nests' of epithelial cells. Typically, these epithelial nests (fragmented cords) lie in proximity to primary follicles [21,22]. In adult ovaries, the SE retains a relatively embryonic structure [25]. The SE-derived cords are in contact or penetrated by nerve terminals, and fragmented cords (nests) are suggested to contribute epithelial elements to ovarian follicles [22].

These data indicate that SE exhibits a high degree of variability, by forming evaginations extending from the ovarian surface and invaginations into the stroma. Also, the crypt-like subsurface channels exist, which are lined by epithelial cells and retain the relatively embryonic structure of SE cells. On the other hand, epithelial nests derived from epithelial cords appear to contribute epithelial cells to ovarian follicles.

Epithelio-mesenchymal transition in vitro

In culture, the ovarian SE cells undergo an epithelio-mesenchymal transition. The resulting mesenchymal type cells can be stimulated to differentiate back into the epithelial phenotype [26,27]. Ovarian SE cells undergoing this epithelio-mesenchymal conversion are initially cytokeratin (CK) positive, but lose CK expression with time and passages in cultures [28]. Therefore, the diminution of CK expression appears to indicate a resting stage for SE-derived mesenchymal cells.

Expression of mitogen-activated protein kinases

Normal SE cells express mitogen-activated protein kinases (MAPK) [29], a group of serine/threonine kinases. The MAPK is used throughout evolution to control the cellular responses to external signals such as growth factors, nutrient status, stress or inductive signals. Transcription factors are substrates for MAPK [30]. In adult human ovaries, we have reported prominent cytoplasmic MAPK expression in oocytes of heathy primary follicles, a diminution of oocyte MAPK expression during follicular atresia, and translocation of cytoplasmic to nuclear MAPK expression in growing secondary follicles [31]. Hence, cytoplasmic MAPK expression appears to be characteristic for resting healthy oocytes. Nuclear translocation signals oocyte growth.

Identification of germ cells in ovarian surface epithelium

Scanning and transmission electron microscopy have revealed numerous germ cells (10 μm in diameter) within the ovarian SE of human fetuses from 7 to 24 weeks of intrauterine life. Germ cells are easily distinguished from smaller coelomic epithelial cells by their rounded contour, smooth surface and, in some instances, large amoeboid evaginations [19]. Using differential interference contrast (DIC) and immunohistochemistry, we previously reported the occurrence of similar putative germ cells within the SE and cortex of adult human ovaries [32]. These data indicate that germ cells are present in the SE. They may either invade SE from adjacent structures and be extruded from the ovary [19], or originate in SE and invade the ovarian cortex, or both [32].

Besides their characteristic morphology as outlined above, the germ cells can also be identified by alkaline phosphatase activity [9]. However, nonspecific alkaline phosphatase activity has been described in various tissues [33-36]. Zona pellucida (ZP) proteins are more specific markers for oocytes. In postnatal rat ovaries, zona pellucidae first appear in primary follicles adjacent to keratin-positive granulosa cells [37]. However, some ZP proteins, such as PS1, are also detected in the ovarian SE of rabbit, cat, monkey, baboon and human, and in human ovarian cancers [38-41]. Hence, expression of ZP proteins in SE cells suggests a relationship to the oocytes.

Intravascular transport of germ cells

Germ cells are capable of migration by amoeboid movements, but in large mammals they also utilize intravascular transport to reach distant destinations [4,42]. Why the cell leaves the circulating blood at certain sites remains unclear. It has been suggested that there is a trapdoor mechanism that prevents the germ cell from continuing to circulate, although adhesion of primordial germ cells ("cauliflower-like structures ") in the aortas of bovine embryos have been observed [42]. Hence, in large mammals, germ cells may migrate to reach adjacent blood vessels, and then utilize vascular transport to reach distant destinations.

Balbiani body

Oocytes in primary (resting) follicles show a single Balbiani body (named for the nineteenth century Dutch microscopist) in the cytoplasmic region near the nucleus where the majority of oocyte organelles are concentrated (reviewed in [43]). The Balbiani body contains aggregated mitochondria and can be observed in primary follicles in both fetal and adult ovaries [44-46]. In a study of turkey hens, no Balbiani body was detected in stage I oocytes, appeared in stage II oocytes, and diminished in the oocytes of growing follicles, coinciding with the dispersion of mitochondria throughout the ooplasm [44].

Similar observations were reported in human oocytes [45]. Balbiani bodies show immunostaining for CK 8,18, and 19 [32,47]. In primary follicles of fetal and adult human ovaries, follicular (granulosa) cell extensions penetrate deep into the ooplasm, much like a sword in its sheath. There may be as many as 3–5 "intraooplasmic processes", even in one scanning microscopy plane. These intraoocytic invaginations are closely associated with a variety of organelles. They are close to the nuclear zone, and may help activate growth of the oocyte [48].

In mouse fetal ovaries, germ cells are arranged in special clusters (germline cysts) and dividing germ cells remain connected by intercellular bridges called "ring canals." The cysts may allow certain germ cells to specialize as nurse cells [49]. One possibility is that such nurse cells in germline cysts help provide oocytes with mitochondria [50]. It has been proposed that mitochondria with functional and defective genomes would be actively transported into different germ cells, and the quality of each cell's mitochondria might then determine whether it survived or entered apoptosis [49]. A recent study by Cox and Spradling indicates that during Drosophila oogenesis, follicular cells are a source of mitochondria, which enter the oocyte cytoplasm via the "ring canal" to form the Balbiani body, thereby supplying virtually all of the mitochondria of the oocyte [46].

It appears that the Balbiani body contributes to the resting state of the oocyte, since oocyte mitochondria are not released until the initiation of the follicular growth. In addition, the contribution of granulosa cells to the formation of the Balbiani body in the oocyte cytoplasm is an indicator of the use of these cells in ongoing oocyte assembly.

Numbers of ovarian primary follicles

In adult mammalian ovaries, 70–95% of oocytes are in various stages of degeneration [51,52]. Block's quantitative morphological investigations of follicles in women [53] showed wide individual variation, but the numbers in the right and left ovaries are similar, with a tendency to decline with age. However, in the eighteen to thirty eight year age range, a relationship between age and the number of primary follicles could not be statistically proven [53]. The number of primary follicles in both ovaries varied between 8100 and 290000. This lack of significant numerical change during the reproductive period also has been reported in cattle [52]. Gougeon used the data of Block and his own observations and concluded that the depletion of the primary follicle pool is caused mainly by atresia in younger women and by a decrease in the growing pool in older women, with the changing point at 38 ± 2.4 years of age [54]. These observations suggest that in human females new cohorts of primary follicles may replace follicles undergoing atresia until about the end of the third decade of life, and a lack of follicular renewal after that period may cause a significant decrease in the pool of resting primary follicles.

We used the immunohistochemical detection of the CK marker of epithelial cells and DIC to study the mesenchymal-epithelial transition of TA mesenchymal cells in adult human ovaries and the development and distribution of epithelial aggregates in the cortex. We also investigated the association of oocytes with cytokeratin positive epithelial nests in ovarian cortex by double color immunohistochemistry, and the expression of SE/oocyte shared ZP proteins and mitogen activated protein kinases in putative germ cells. In addition, triple color immunohistochemistry was employed on serial sections to study vascular involvement in oocyte transportation. This study expands our earlier and recent observations and views on the formation of germ cells in adult human ovaries [31,32,55,56]. Our present data support further the concept of the formation of new ovarian primary follicles during the optimal reproductive period in human females.

Materials and methods

Tissues

Morphological and immunohistochemical observations from human ovaries presented here come from the material collected over 12 years. Tissue samples from ovaries and other reproductive tract tissues were obtained from over 100 women undergoing hysterectomies. In the present study we report the data obtained from ovarian samples of women during the optimal reproductive period of life. Hysterectomies are relatively uncommon in these women (chronic pelvic pain, not responding to the conservative treatment). We here report observations from the ovaries of twelve patients (mean age 32.8 ± 4.1 SD, range 27–38 years; 41 tissue samples). All cases showed functional or regressing CL in the ovaries and corresponding type of endometrial morphology, indicating regular ovulatory cycles. The study was approved by the Institutional Review Board, and a written consent was obtained from each patient.

Peroxidase immunohistochemistry

Tissue processing began within 30 minutes of surgery. Up to four 10 × 10 × 5 mm blocks of tissue were collected from each ovary. Tissue blocks of ovarian samples were frozen in optimal cutting temperature (O.C.T.) compound (Miles Inc., Elkhart, IN) and stored at -80°C until use. Under these conditions, no differences in immunohistochemical staining were detected when the same tissue blocks were processed within one month after embedding or ten years later. Twenty to sixty (and occasionally more) frozen sections (7 μm thickness) were fixed in acetone and processed for detection of markers of

interest by peroxidase immunohistochemistry as described previously [32]. Immunohistochemical evaluation was performed by two investigators (A.B. and M.S.). All chemicals, except where specified otherwise, were purchased from Sigma Chemical Co., St. Louis, MO, USA.

Double color immunohistochemistry

The slides were subjected to double color immunohistochemistry for CK and ZP immunoreactivity (CK/ZP). The slides were first immunostained for CK of epithelial cells and TA fibroblasts, but without hematoxylin counterstain and dehydration. Briefly, specimens were washed with phosphate buffered saline (PBS) and incubated 20 minutes with mouse-anti human CK 18, clone CY-90 (Sigma) or CK 5, 6, 8, 17, clone MNF116 (Dako Corporation, Carpinteria, CA, USA) (5 μg/ml in PBS). After extensive washing in PBS, specimens were incubated 20 minutes with swine anti-mouse IgG peroxidase conjugate (SwAM/Px; SEVAPHARMA, Prague, Czech Republic – kindly provided by Dr. Jana Peknicova, Department of Biology and Biochemistry of Fertilization, Institute of Molecular Genetics, Academy of Sciences of the Czech Republic, Prague, Czech Republic) diluted 1:50 and preabsorbed with rat kidney homogenate [57]. Antigen-antibody complexes were detected by a standard diaminobenzidine technique (brown color).

After three washes in PBS, the slides were incubated for 20 minutes with rabbit antibody to heat-solubilized porcine zona (HSPZ) [58,59], diluted 1:20, or sheep antibody to heat-solubilized rabbit zona (HSRZ) protein [59] (1:20), or PS1 monoclonal antibody to the meiotically expressed porcine oocyte ZP carbohydrate antigen [38] (1:100). The antibodies were kindly donated by Dr. Bonnie S. Dunbar, Department of Molecular and Cellular Biology, Baylor College of Medicine, Houston, Texas, USA. Additional rabbit anti-HSPZ antibodies [58] were kindly provided by Dr. Satish K. Gupta, National Institute of Immunology, New Delhi, India. The following monoclonal primary antibodies were also utilized at IgG concentration 5 μg/ml: CD31 of endothelial cells, clone JC/70A (Dako Corporation, Carpinteria, CA, USA), HLA-DR of endothelial cells and activated tissue macrophages, clone MEM-12 [60] (Drs. Ivan Hilgert and Vaclav Horejsi, Institute of Molecular Genetics, Academy of Sciences of the Czech Republic and Faculty of Sciences, Charles University, Prague, Czech Republic), MAPK (pan-ERK), clone 16 (BD Transduction Laboratories, San Diego, CA, USA), and Thy-1 differentiation protein of fibroblasts and pericytes, clone F15-42-01 [61] (Dr. Rosemarie Dalchau, Institute of Child Health, University of London, London, UK).

Primary antibodies were followed by a relevant peroxidase-coupled secondary antibody – AffiniPure Goat Fab' Anti-Rabbit IgG (H+L), Abs. human serum (Protos Immunoresearch, Burlingame, CA, USA) and AffiniPure Rabbit Anti-Sheep IgG, Fc Fragment Specific – minimal cross-reaction to Human Serum Proteins (Jackson Immunoresearch Laboratories, West Grove, PA, USA), or SwAM/Px (SEVAPHARMA) as above. Antigen-antibody complexes were detected by a Vector SG detection kit according to the supplier's manual (Vector Laboratories, Inc., Burlingame, CA, USA), giving the substrate dark blue color. This contrasted with the brown color resulting from the first sequence of immunoreagents (CK immunostaining). The slides were dehydrated and mounted, without hematoxylin counterstain. A control procedure consisted of double color immunohistochemistry as above, but both primary antibodies were replaced with PBS. Additional controls included replacement of primary antibodies with nonimmune hybridoma ascites, antibodies not reacting with human tissues (mouse-anti rat Thy-1 differentiation protein, clone OX-7 – donated by Dr. Allan F. Williams, MRC Cellular Immunology Unit, Sir William Dunn School of Pathology, University of Oxford, Oxford, UK), and normal rabbit IgG.

Since the diaminobenzidine reaction product masks the antigen and catalytic sites of the first sequence of immunoreagents, preventing interaction with the reagents of the second sequence [62], a possibility of co-expression in the same cell types was investigated. Therefore, another set of slides was similarly processed, with the opposite order of primary antibodies (ZP/CK). In addition, two sets of slides were immunostained for CK or ZP expression alone, followed by hematoxylin counterstain.

Triple color immunohistochemistry

Double color immunohistochemistry was performed as above and complemented with the third primary antibody and corresponding secondary antibody incubation. Antigen-antibody complexes were detected by a Vector VIP detection kit according to the supplier's manual (Vector Laboratories), giving the substrate a purple color. Control staining consisted of the same procedure, but primary antibodies were replaced as indicated above.

Differential interference contrast images were captured with a DEI-470 CCD Video Camera System (Optronics Engineering, Goleta, CA) with detail enhancement and CG-7 color frame grabber (Scion Corporation, Frederick, MD) supported by Scion Image public software developed at the National Institutes of Health (Wayne Rasband, NIH, Bethesda, MD). Captured images were compiled using Microsoft® Power-Point® 97 SR-2 (Microsoft Corporation, Redmont, WA) and Microsoft Photo Editor 3.0 (Microsoft Corporation).

Statistics

Statistical analysis of data on primary follicle numbers from Block [53,63,64] and Gougeon et al. [54] was performed using GraphPad InStat version 3.01 for Windows software (GraphPad Software, San Diego, CA). The follicle count values were transformed (Y = Log [Y]) and subjected to One way Analysis of Variance (ANOVA) followed by Tukey-Kramer Multiple Comparisons Test. Probability values of $P < 0.05$ were considered significant.

Results

Presentation of data does not necessarily follow the outline given in the background, but rather the development of our approach and methodological analysis of the problem. Also, due to the complexity of views and approaches, some subheadings include a short discussion and conclusions.

It is important to note that the single color immunohistochemistry has an advantage in showing a marker distribution as it is. In double color immunostaining, the markers of second sequence may not be visible if they are expressed in cells also showing strong expression of the first sequence marker. For instance, if the expression of CK and ZP proteins is shared in some SE cells, the CK immunostaining used for the first sequence is visible and ZP proteins are masked. Co-localization of ZP and CK immunostaining is also common in granulosa cells of primary and secondary follicles (data not shown). This, however, does not apply to germ cells and oocytes, which express ZP but not CK markers. In each figure with double and triple color immunostaining the sequence of antibodies is indicated. In this study, the blocking effect of the primary antibody sequence in cells sharing both markers is in fact an advantage of peroxidase immunohistochemistry, giving a clear distinction between CK+/ZP+ granulosa cells and CK-/ZP+ oocytes. In addition, this technique shows that during follicular growth some granulosa cells are depleted of CK immunoexpression but ZP staining persists (see Fig. 11D).

Relationship of tunica albuginea, surface epithelium and ovarian cortex (Fig. 1 and 2)

In most instances, the ovarian cortex was covered by TA, with or without a surface epithelium cover. The TA showed a variable thickness, ranging from almost undetectable to more than 50 μm. Cytokeratin expression of various density was detected in mesenchymal cells of some TA segments, particularly in segments showing an appearance of SE cells. In contrast, no CK expression was detected in mesenchymal cells of the ovarian cortex.

A panoramic view of events at the ovarian surface resulting in the development of cortical channels and epithelial cords is presented in Fig. 1A. This process is initiated by the appearance of SE cells directly connected to the ovarian cortex (dotted box, Fig. 1A). The segments of SE cells (arrow) are gradually overgrown by TA flap (arrowhead). This results in the formation of SE channels with lumen (se-ch, inset) and solid epithelial cords (white arrow). Note a lack of ovarian SE above the TA (white arrowhead).

A high power view of the TA flap extending over the SE (Fig. 1B, detail from 1A) revealed strong CK expression (brown color) in mesenchymal cells exhibiting fibroblast morphology (+fb). Such cells associate with the inner flap surface covering the SE (arrowhead). At the angle between the flap and SE, the cells show intermediate morphology of fibroblasts and epithelial cells (fb/se), and appear to contribute to the SE cover of the ovarian cortex (arched arrow). Solid epithelial cords (Fig. 1C, detail from 1A) show a CK+ bilaminar epithelial layer accompanied by a diminution of CK immunostaining of adjacent TA fibroblasts (+/-fb).

Figure 1D, a panoramic view of the ovarian surface and adjacent cortex from another case, shows a thick segment of TA and CK expression in TA fibroblasts associated with the differentiation of SE (left white arrow). No SE is apparent above TA lacking CK+ fibroblasts (right white arrow). The upper ovarian cortex contains a row of longitudinally (arrows) or perpendicularly viewed epithelial cords (arrowheads), evidenced from serial sections.

Segments with TA hypertrophy and without an SE cover showed strong CK expression in TA fibroblasts (fb, Fig. 2A). No CK expression was detected in the adjacent ovarian cortex (Fig. 2B). The CK+ fibroblasts migrate toward the surface (Fig. 2C) and show the mesenchymal-epithelial transition (fb/se, Fig. 2D) similar to that observed in the TA flap (Fig. 1B). The appearance of SE cells was associated with a gradual diminution of CK expression by TA fibroblasts (Fig. 2E; arrowhead, Fig. 2F). Well differentiated SE was eventually underlined by an amorphous substance without cellular components (white arrowhead, Fig. 2F). Such separation of the SE from cellular components of TA may cause a sequestration of the nonessential SE out of the ovary.

Taken together, these observations indicate that TA fibroblasts, which show a transient CK immunoexpression, differentiate into SE cells by a process of mesenchymal-epithelial transition. However, depending on additional (unknown) factors, this process may result either in the formation of SE channels and cords in the ovarian cortex, or in the differentiation of SE cells covering the ovarian surface.

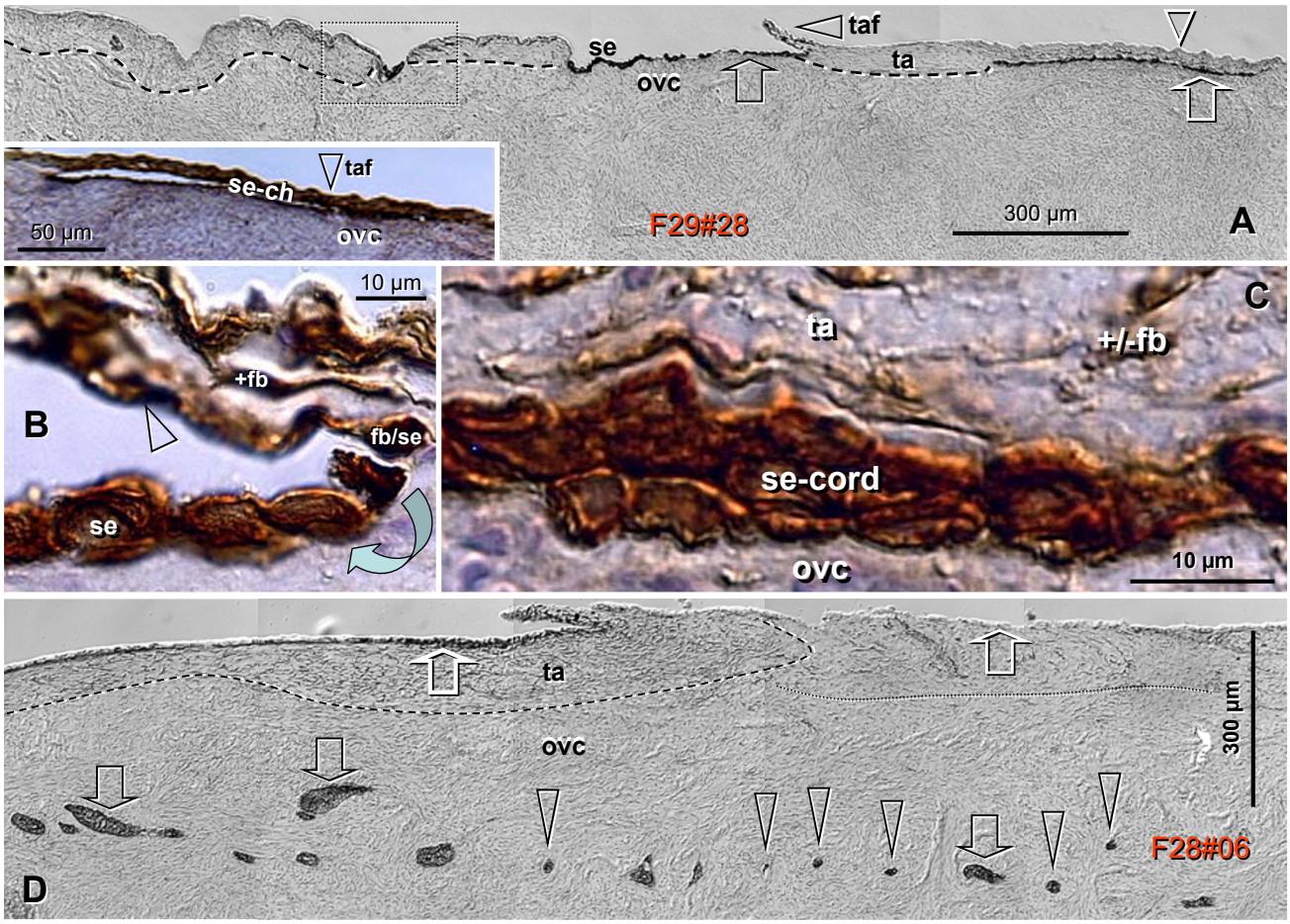

Figure 1

Formation of epithelial cords from ovarian TA mesenchymal precursors - see also Ref [32]. A) Panoramic view of ovarian surface and adjacent cortex. Dashed line indicates interface between TA and stroma of the ovarian cortex. Dotted box indicates an early appearance of SE cells adjacent to the ovarian cortical stroma. Inset, epithelial channel (se-ch); se and arrow, surface epithelium cells; taf and arrowhead, TA flap; white arrowhead – a lack of SE cells above the TA; white arrow -bilaminar epithelial cord. **B**) Detail from (**A**) shows association of CK+ (brown color) fibroblasts (+fb,) with the TA flap surface (arrowhead), and transition from mesenchymal to epithelial morphology (fb/se) and surface epithelium cells (se, arched arrow). **C**) Detail from (**A**) shows CK+ epithelial cord consisting of two layers of epithelial cells and lying between the ovarian cortex (ovc) and TA. Note diminution of CK immunoexpression in TA fibroblasts (+/-fb). **D**) Parallel (black arrows) and perpendicular (arrowheads) view of epithelial cords in the upper ovarian cortex (ovc). Dashed line indicates a segment of CK+ TA with flap and differentiating SE cover (left white arrow). Dotted line indicates CK- segment lacking SE cower (right white arrowhead). F29 indicates female age in years; #28 = case No. Bar in (C), for (B and C). Cytokeratin 18 immunostaining (brown color) and hematoxylin counterstain.

Rows of ovarian epithelial cords in the upper cortex are accompanied by rows of primary follicles in the lower cortex (Fig. 3)

Figure 3 shows formation of epithelial channels (arrowhead), longitudinally (dashed arrowhead) and perpendicularly viewed solid epithelial cords (white arrowheads and right inset), and follicle like structures containing stromal elements (solid box, see left top inset for detail) in the upper cortex (uc). These structures were arranged in a surprisingly straight row (see also Fig. 1D). In some ovaries a similar orientation of primary follicles was observed in the lower ovarian cortex (Ic).

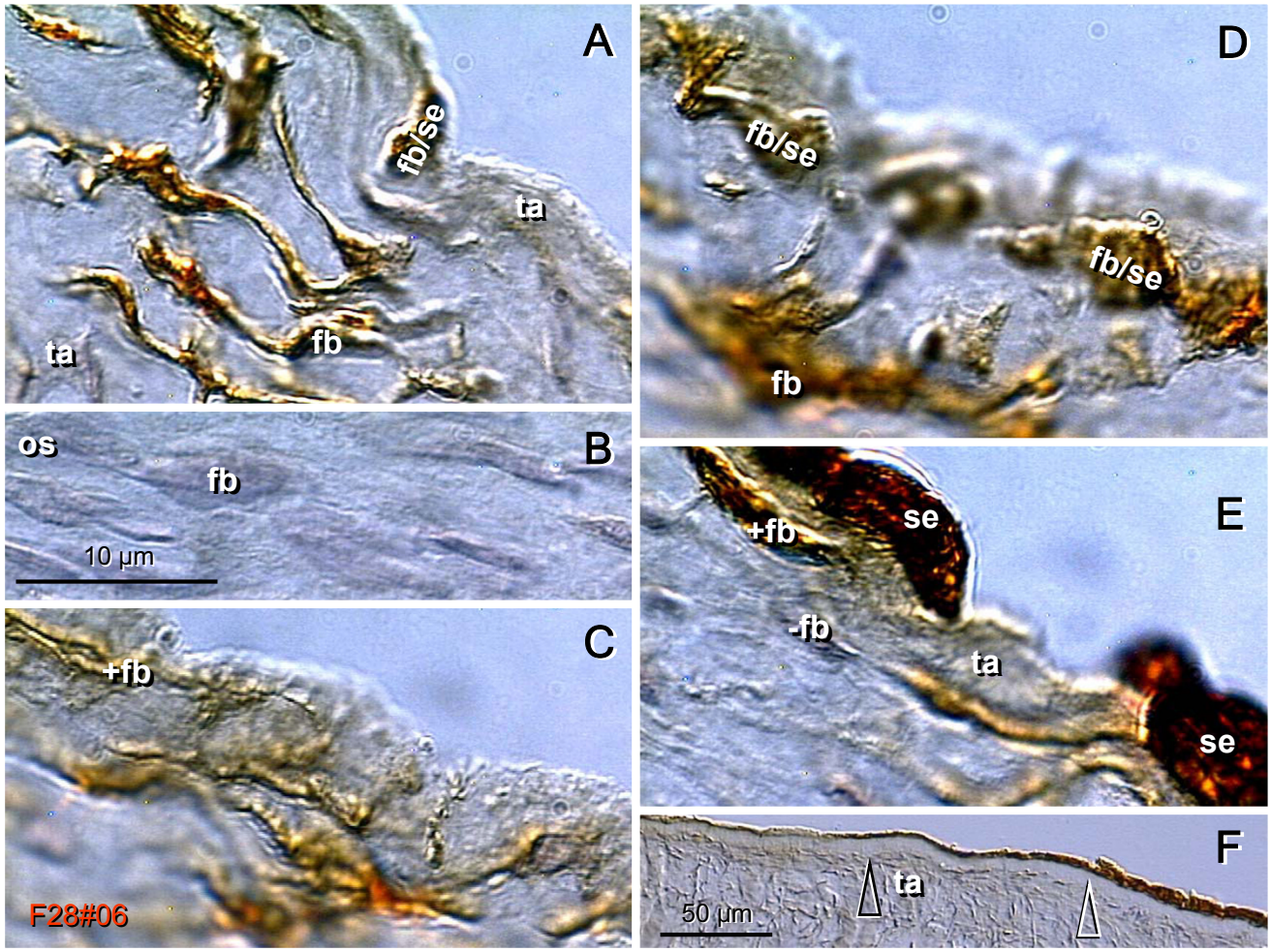

Figure 2
Formation of ovarian SE from TA mesenchymal precursors. A) Tunica albuginea (ta) fibroblasts (fb) showing strong CK immunoexpression (brown color). One cell in mesenchymal-epithelial transition is apparent at the surface (fb/se). **B**) Ovarian stroma (os) shows no CK staining of fibroblasts (fb). **C**) Fibroblasts associated with the TA surface exhibit mesenchymal-epithelial transitory forms (**D**). **E**) Appearance of SE cells (se) is associated with a diminution of CK immunoexpression (-fb). F) Differentiation of the SE is associated with a diminution of cellularity in adjacent TA. Bar in (B), for (A-E). Cytokeratin 18 immunostaining, hematoxylin counterstain.

Epithelial nests assemble with oocytes to form new primary follicles (Fig. 4 and 5)

As pointed out in the Background, studies of Motta et al. [21,22] have shown that in some areas of the ovary epithelial cords fragment and appear as small nests of epithelial cells which lie in proximity to primary follicles [22]. In order to study the possible formation of new follicles from epithelial nests and oocytes, we used cytokeratin staining to view the nest (primitive granulosa) cells and DIC to study unstained oocytes. In the lower ovarian cortex, some epithelial nests were found associated with the lumen of ovarian venules. Figure 4, panels A and B (copy of A completed with symbols) shows a venule lumen (vl) lined by endothelial cells (e) and a CK+ epithelial nest wall (w). The nest shows an arm (a) associated with the putative oocyte (o) and possibly migration of the oocyte outside of the vascular lumen.

Ongoing assembly of the epithelial nest with an oocyte is shown in Fig. 4, panels C and D. The nest exhibits closing "gates" (g). A small portion of the oocyte (dashed line), which still lies outside, is expected to join the complex (arched arrow). Note that the nuclei of stromal cells are visible through the oocyte tail, which may be less thick

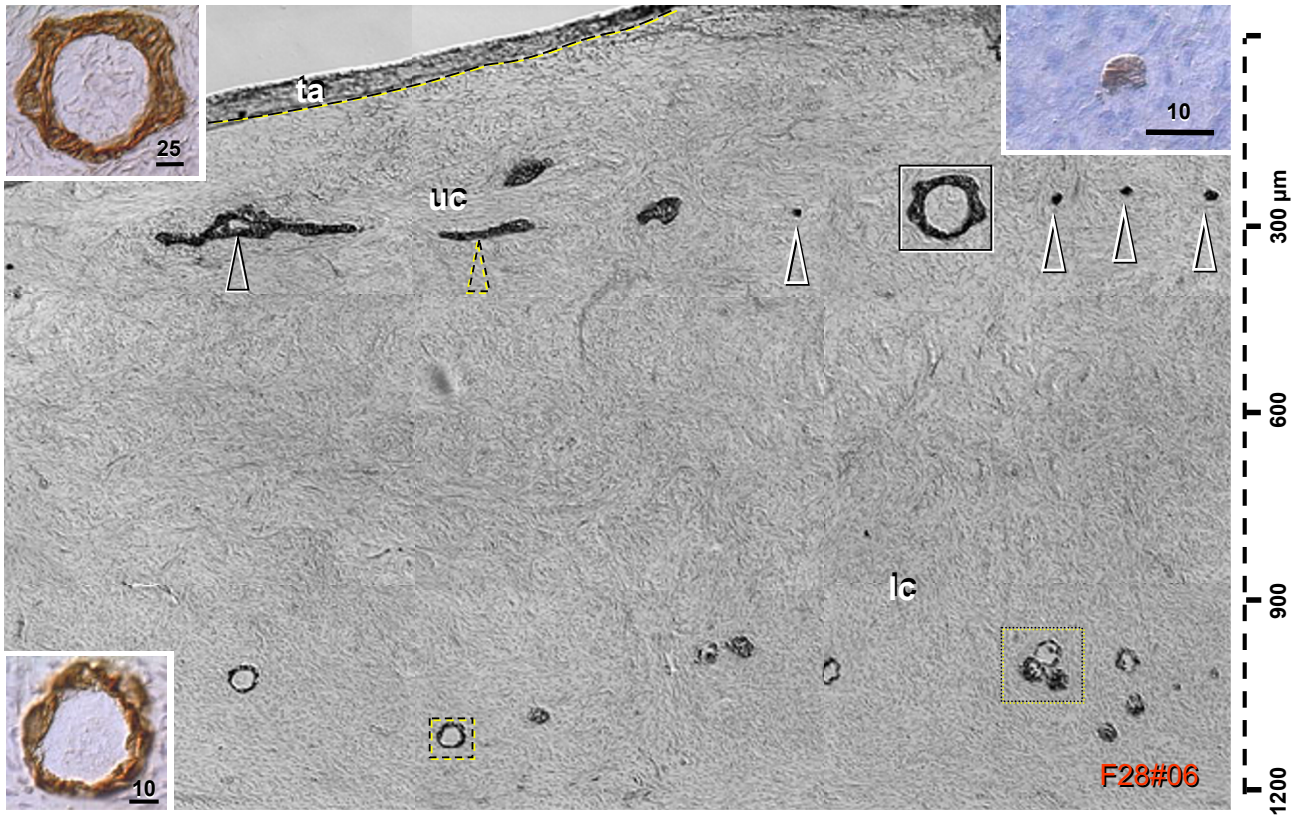

Figure 3
Distribution of epithelial cords and primary follicles in the ovarian cortex. Panoramic view composed of nine images shows ovarian tunica albuginea filled with CK18+ mesenchymal cells, upper cortex (uc) with epithelial channels (black arrowhead), cords (dashed and white arrowheads – see right inset) and follicle-like structures (solid box, see upper left inset for details). Lower cortex (lc) shows isolated (dashed box – see lower left inset) and grouped primary follicles (dotted box). Bars in insets indicate µm. Cytokeratin 18 immunostaining, hematoxylin counterstain.

than the 7 µm thickness of the cryostat section. Cytokeratin+ projections from the nest wall into the oocyte cytoplasm (arrows) appear to contribute to the formation of the Balbiani body (asterisk) adjacent to the oocyte nucleus (dotted line). Perpendicularly-viewed CK+ projections of nest cells reaching the paranuclear space are indicated by arrowheads.

Various stages of the oocyte-nest assembly are shown in Fig. 5A [note adjacent dilated venule (v)], and magnifications 5B-D. Panel B (arrow, panel A) shows an oocyte at the midpoint of the assembly with the nest. The nest gate flaps (g) are inverted inside. No Balbiani body is apparent, and CY+ extension from nest cells reaches the oocyte nucleus (black arrowhead). Another CY+ extension is in contact with the oocyte nucleolus (x), which shows traces of circumferential CK staining (white arrowhead). A more advanced stage of oocyte-nest assembly is shown in panel C (white arrow, panel A). The oocyte nucleus adjacent to the nest wall (w), just opposite the closing nest gate (cg), is embraced by "intraooplasmic processes" (arrows) from the nest cells. The Balbiani body (asterisk) appears to reside within the oocyte nucleus. Completion of the oocyte-nest assembly is shown in panel D (arrowhead, panel A). The former nest gate ('g') is closed, and the Balbiani body lies within the oocyte cytoplasm, between the oocyte nucleus and the nest wall. The oocyte nucleus is free of CK staining. A thick intraooplasmic extension from the nest cells is also apparent (arrow). Panel D also shows the top of an adjacent follicle (ft).

Double color immunohistochemistry (Fig. 6 and 7)
In order to better visualize assembly of oocytes with epithelial nests, we used double color

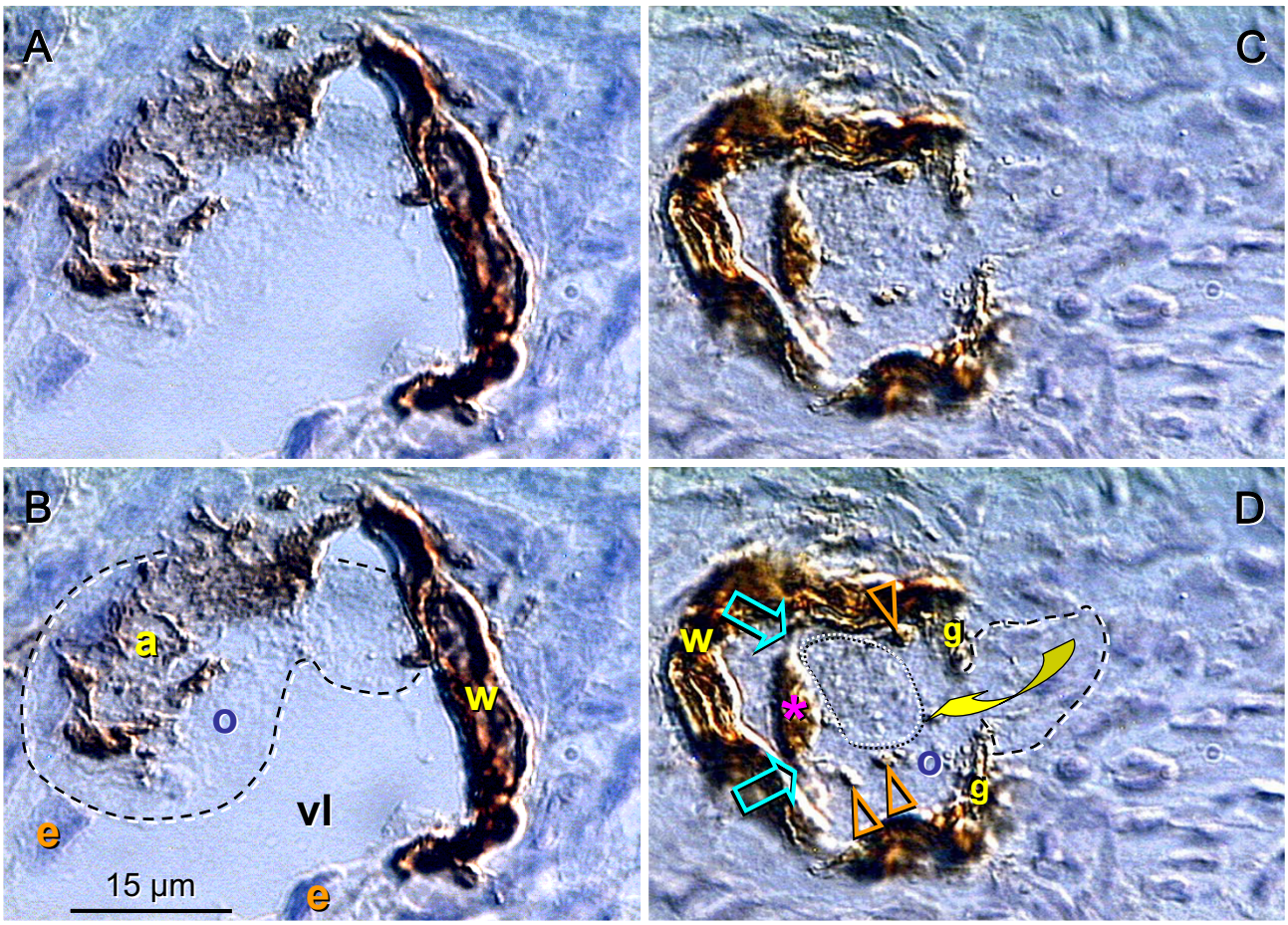

Figure 4
Association of epithelial nests with cortical vessels, oocyte-nest assembly and formation of CK18+ Balbiani body. A and **B** (copy of **A** with letters and dashed line) show the CK+ (brown color) nest body wall (w) inside of the cortical venule, which extends an arm (a) to catch the oocyte (o, dashed line) and move it outside of the blood vessel. **C** and **D** show the nest body and closing "gate" (g). A portion of the oocyte (dashed line) still lies outside of the complex, and is expected to move inside (arched arrow). The oocyte contains intraooplasmic CK+ (brown color) material (arrowheads). Extensions from the nest wall (arrows) contribute to the formation of CK+ paranuclear (Balbiani) body (asterisk). The oocyte nucleus is indicated by a dotted line. vl, vascular lumen; e, endothelial cells. CK18 immunostaining, hematoxylin counterstain.

immunohistochemistry for CK and ZP proteins. These sections were not counterstained with hematoxylin, but enhanced DIC has been used. Fig. 6A shows an association of the oocyte (blue ZP immunoexpression) with epithelial nest (brown CK immunoexpression) resembling an occupied bird's nest. This phase of assembly is similar to that shown in Fig. 5B. An earlier stage is shown in Fig. 6B, where the CK+ nest (brown color) shows octopus-like shape with multiple CK+ trunks embracing the ZP+ (blue) oocyte.

An association of the oocyte-nest assembly with cortical vasculature is presented in Fig. 7, which shows four serial sections (7 µm each) from the ovary of another woman. In panel A (the bottom of the oocyte-nest assembly), CK+ (brown) ramifications of an epithelial nest lie inside the vessel (v) showing focal ZP (blue) staining (arrowhead) in the vascular wall. The next serial section (panel B) shows a spot of ZP staining (arrowhead) among the nest ramifications associated with a "harboring" oocyte nucleus (n). The insets show that putative tadpole-like germ cells (presumptive surface indicated by the dashed and nucleus by the dotted lines), which have been found among dense

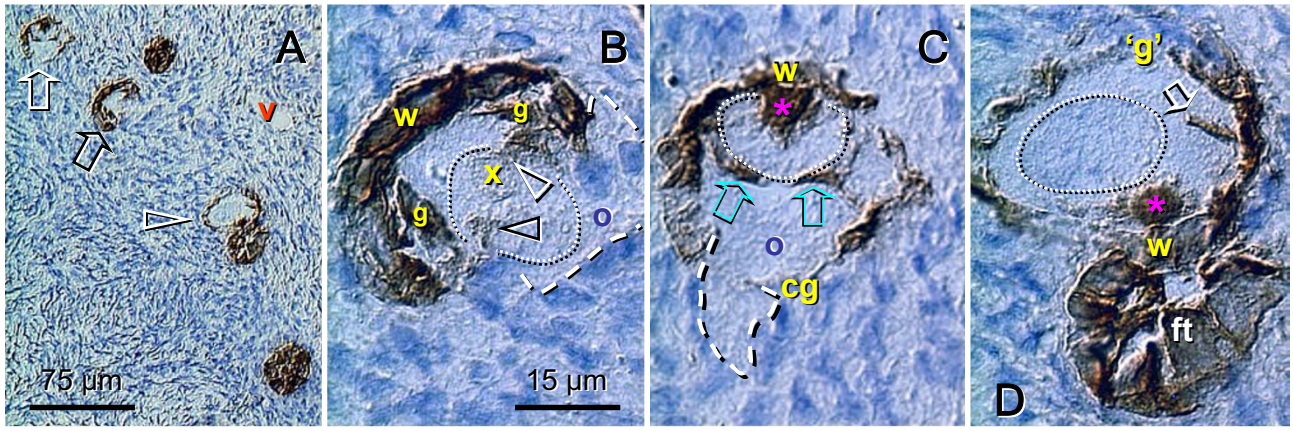

Figure 5
Sequential stages of the oocyte-nest assembly and Balbiani body formation. A) A group of primary follicles in various stages of formation. Note adjacent venule (v). **B**) Early stage (see arrow in A) shows the oocyte during entrance into the CK+ (brown color) nest with nest wall (w) and inverted "gates" (g). Cytokeratin+ material appears to enter the nucleus (black arrowhead) and traces (white arrowhead) are visible around the nucleolus (x). Note a lack of Balbiani body. **C**) More advanced stage (white arrow in A) shows the oocyte nucleus (dotted line) adjacent to the nest wall (just opposite to the closing gate), embraced by intraooplasmic extensions (arrows). The Balbiani body (asterisk) appears to reside within the nucleus (dotted line), and small proportion of the ooplasm (dashed line) is still outside of the complex. D) Completed formation of primary follicle (arrowhead in A) shows closed gate ('g'), CK+ Balbiani body at the opposite side, adjacent to the nest wall, oocyte nucleus free of CK staining, and a single CK+ intraooplasmic extension (arrow) from the nest side. A follicle top (ft) from an adjacent follicle is also visible. CK18 immunostaining, hematoxylin counterstain.

fibroblasts in the upper ovarian's cortex [32], exhibit ZP expression (blue) in the intermediate section of the cell (arrowhead), between the heading nucleus and the tail.

The next serial section (panel C) shows CK+ sword-like projections (yellow arrowheads) from the nest wall (w), one of which penetrates the oocyte's intermediate section (is) toward the oocyte tail (t). Note a CK+ "eye" (orange arrowhead) in the oocyte's intermediate section (see also insets in panel D). There are also anchor-like projections from the oocyte (blue arrowhead) toward the vascular wall, possibly contributing to the ZP staining in the adjacent stroma (arrow). The top of the complex (panel D) shows a flap of the vascular pocket (vp) with anchor-like CK+ and ZP+ projections (arrowheads). Segments of the intermediate section of the oocyte and the tail are still visible. Insets show the putative tadpole-like germ cell (dashed line) associated with the vasculature (v) in the upper ovarian cortex. Note larger size compared to insets in panel B, and appearance of CK+ "eye" (arrowhead) of unknown significance in the center of the intermediate section.

Triple color staining (Fig. 8)
To study the association of oocyte-nest assemblies with cortical vessels, we used double color staining as above, complemented with third color for the CD31 marker of vascular endothelial cells. All panels in Fig. 8 are from the same section subjected to the triple color immunohistochemistry. Strong CD31 immunoexpression (purple color) of the luminal aspects of endothelial cells was observed in ovarian medullary vessels (arrowhead, panel A), but not cortical vessels, which showed less dense granular staining of endothelial cells (arrowhead, panel B). Panel C shows the same vessel as in (B), and a derived (arched arrow, as evidenced from serial sections) vascular "pocket" (vp, see Fig. 7D) with endothelial cells (arrowheads) embracing CK+ (brown) nest walls (w) and a ZP+(blue) segment of the oocyte (o). Panel E, copy of (D) with symbols, shows the vascular lumen (vl) encircled by endothelial cells (red arrowhead) and an adjacent follicle top (ft, as evidenced by serial section). Also adjacent is a nest wall (w) extending the CK+ arms (yellow arrowheads) to "catch" the oocyte from the vascular lumen. The blue arrow indicates ZP+ oocyte extensions anchored to the vascular wall.

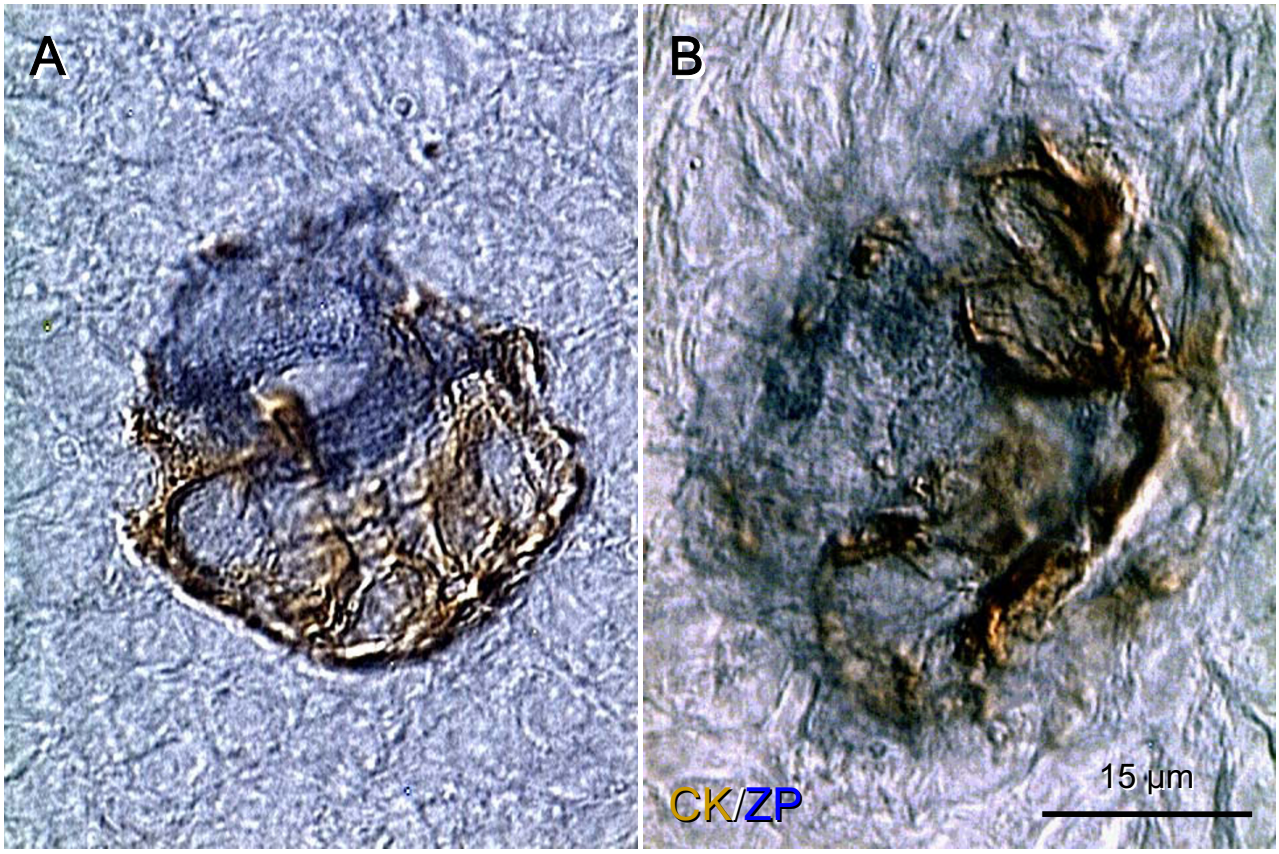

Figure 6
Double color immunohistochemistry of the oocyte-nest assembly. A) Occupied "bird's" nest type indicates a half way oocyte-nest assembly. B) An earlier stage of assembly shows the oocyte embraced by nest trunks, resembling an octopus. Immunostaining with CK monoclonal antibody, clone MNF116 (recognizing CK5, 6, 8, 17) – first sequence visualized with diaminobenzidine (brown color), and with HSPZ (zona pellucida) polyclonal antibody – second sequence visualized with SG (blue color). No hematoxylin counterstain.

PS1 and MAPK immunoexpression during differentiation and migration of germ-like cells (Fig. 9 and 10)

Most of the ovarian SE cells showed CK immunoexpression, but immunoexpression of ZP antigens (PS1, HSPZ and HSRZ) was restricted to certain SE segments. While HSPZ and HSRZ were also detected in the zona pellucida of oocytes during and after assembly within epithelial nests (including primary, secondary, preantral and antral follicles), the PS1 expression was not detected in zona pellucida of oocytes in human ovarian follicles. The PS1 is a meiotically expressed porcine oocyte carbohydrate antigen [40]. It is also found in some human ovarian cancers – unpublished data and [39].

Immunoexpression of PS1 in human SE cells was cytoplasmic. However, cells descending from the SE into TA showed nuclear PS1 (brown) staining (arrows, Fig. 9A). The dividing SE cell, indicated by a red arrow in panel A, shows an asymmetric distribution of meiotically expressed nuclear PS1, suggesting asymmetric division and meiotic activity of the PS1 + daughter cell. Double color immunostaining for PS1 (brown) and CK (blue) also revealed an asymmetric distribution of PS1 in putative germ cells descending from the SE (panels B and C) – note CK+ (blue arrowheads) and PS1+ (brown arrowheads) daughter cells. Larger germ-like cells with nuclear PS1 staining were detected in TA (panel D). Such cells divided (arrow, panel E) and entered the adjacent ovarian cortex (white arrow). In the cortex, the putative germ cells showed a translocation of nuclear PS1 immunoexpression to cytoplasmic staining, suggesting termination of the meiotic prophase, and an association with

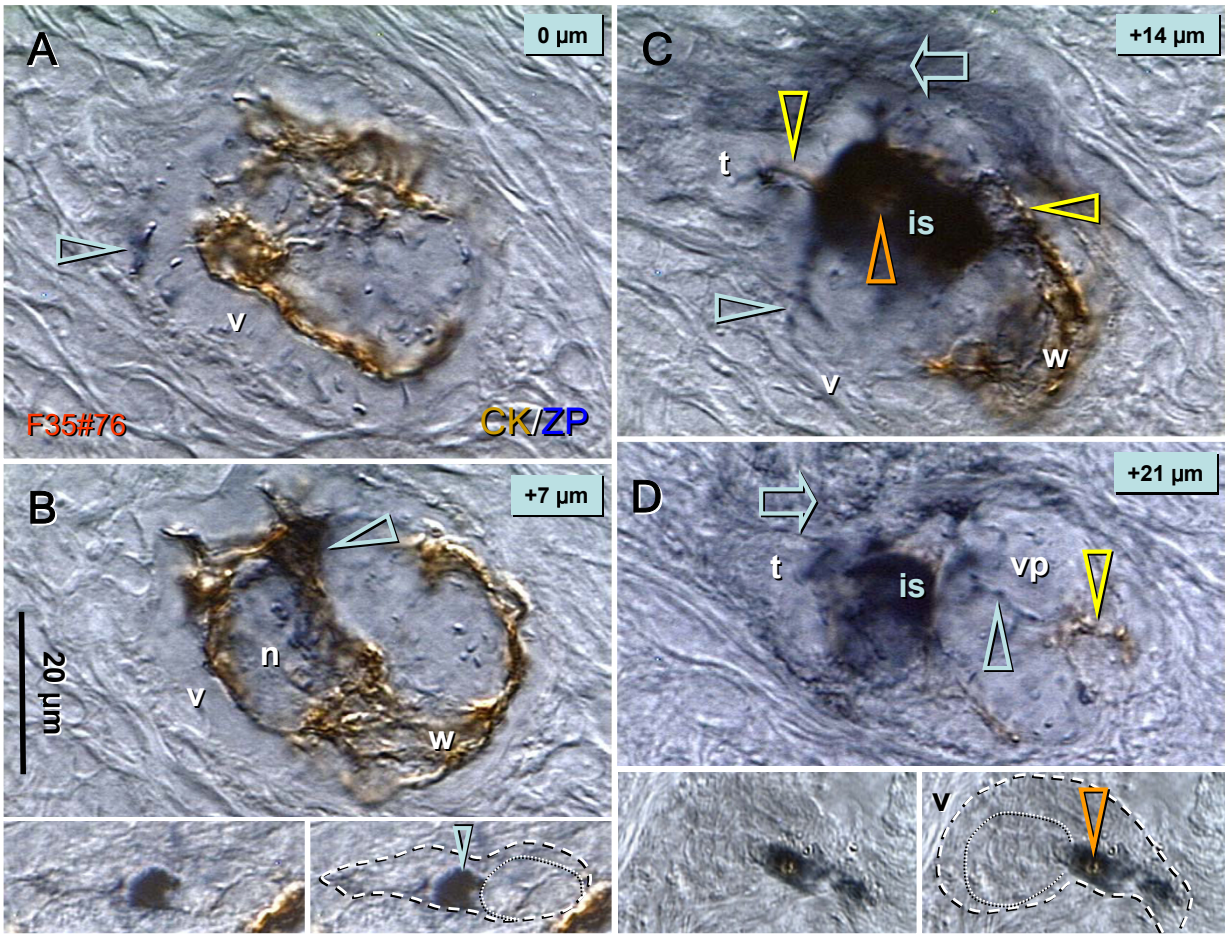

Figure 7
Serial sections through the intravascular oocyte-nest assembly. Serial sections (7 µm thick) through the oocyte-nest assembly show bottom of the complex (**A**); oocyte nucleus (n) plane (**B**); intermediate section (is) and the tail (t) plane (**C**); and top of the complex (**D**). v, vascular wall; vp, vascular pocket; blue arrowheads, ZP+ extensions from the oocyte intermediate section – anchors to the vascular wall; yellow arrowheads, nest extensions penetrating the ooplasm; blue arrows, ZP+ staining (oocyte signaling). Insets in panel B show putative germ cell with ZP+ intermediate section (arrowhead) migrating in the upper ovarian cortex. Insets in panel D show an association of putative germ cell with a cortical vessel (v) wall – note ZP+ intermediate section containing a CK+ "eye" (arrowhead). Details in text. Immunostaining with CK18 (brown color) and HSPZ (blue color). No hematoxylin counterstain.

cortical vasculature showing minute amounts of PS1 immunoexpression in adjacent endothelial cells (panel F). In addition, PS1 immunoexpression (brown color) was detected in germ-like cells descending from CK+ (blue) epithelial crypts into the ovarian cortex (arrow, panel G). No accumulated germline type cells resembling persistence of fetal oogenesis (germline cysts) have been detected.

Staining for MAPK revealed dividing germ-like cells in TA with prominent nuclear MAPK immunoexpression (brown color, Fig. 10A), similar to those showing nuclear staining for PS1 (see Fig. 9E). However, nuclear MAPK immunoexpression persisted in putative germ cells in the upper ovarian cortex (panel B). Intravascular germ-like cells (panel C) showed an increase in size (20 µm) accompanied by an appearance of MAPK cytoplasmic clusters (c) in addition to persisting nuclear MAPK immunoexpression (dotted line). During association of oocytes

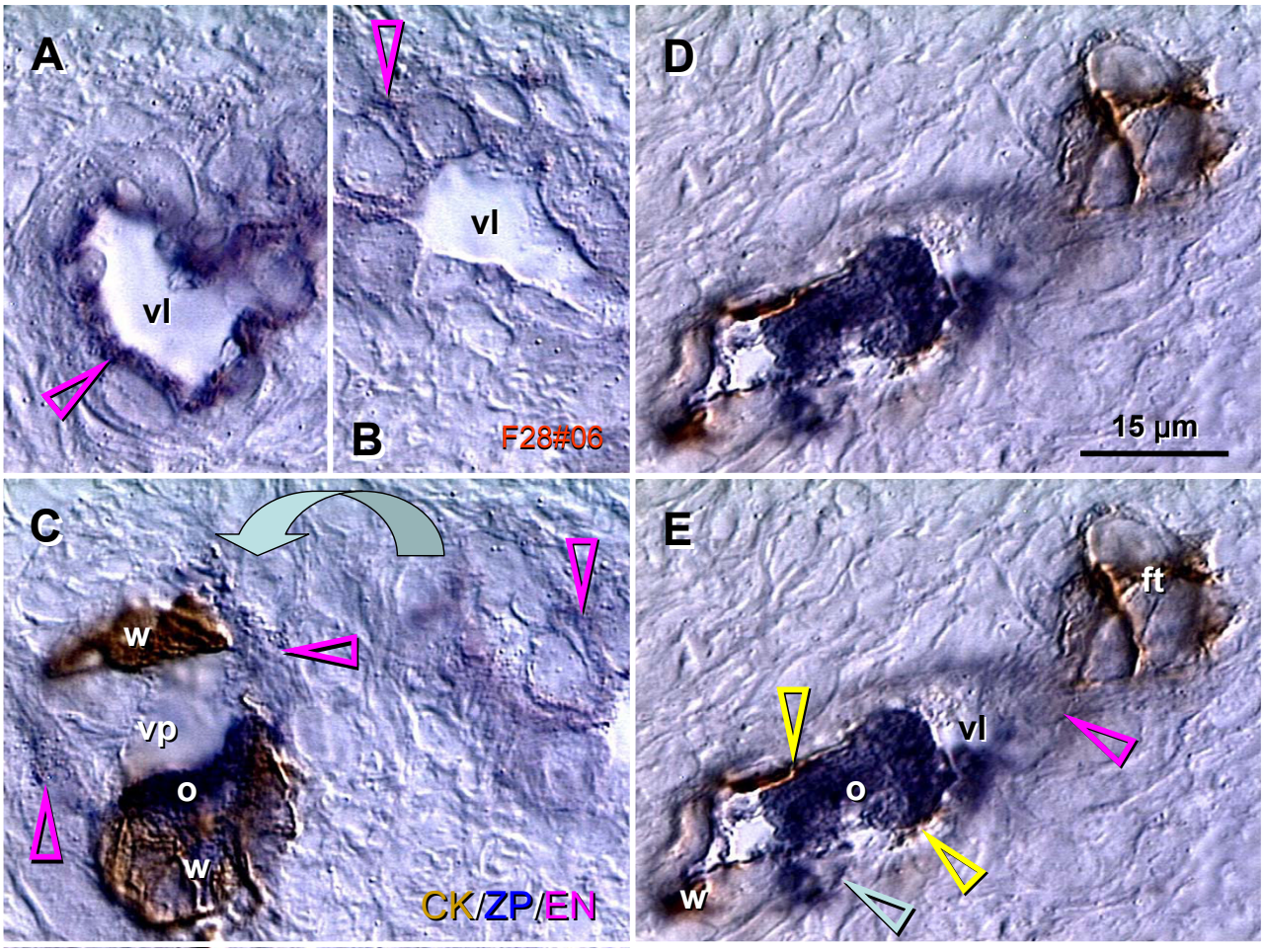

Figure 8
Triple color immunohistochemistry for vascular route of the oocyte-nest assembly. Immunostaining CK/ZP/EN with CK18 (brown color), HSPZ (blue color), and endothelial CD31 – third sequence visualized with VIP(purple color). **A**) Medullary vessels show strong CD31 immunostaining (arrowhead), contrasting weak immunoexpression in cortical vessels (**B**). **C**) in the area adjacent to (**B**) (arched arrow) the vascular "pocket" (vp) shows adjacent endothelial cells, CK+ nest walls (w), and a ZP+ intermediate segment of the oocyte (o). Panels **D** and **E** show vascular wall (red arrowhead) with a lumen (vl) containing ZP+ oocyte "caught" by CK+ extensions (yellow arrowheads) from the nest wall (w). ft, follicle top of an adjacent primary follicle. No hematoxylin counterstain.

(panel D) with CK+ nests (see serial section in panel E) in the lower ovarian cortex, abundant MAPK immunoexpression was apparent in the oocyte nucleus and cytoplasm. Fresh follicles with an established ring of granulosa cells in the adjacent ovarian cortex, showed strong nuclear and cytoplasmic staining but poor MAPK immunoexpression in the paranuclear (Balbiani) body (dashed line, panel F). Panel G shows a low power magnification of follicles presented in panels D-F. The "s" arrow indicates orientation toward the ovarian surface.

Altogether, these observations indicate that germ cells exhibiting nuclear meiotically expressed PS1 oocyte carbohydrate antigen differentiate by asymmetric division from SE cells, divide symmetrically, and complete the first meiotic prophase. These cells exhibit abundant nuclear MAPK immunoexpression, indicating activation of signaling pathways resulting in lineage commitments into certain cell types [65] (see below). No accumulated germline type cells (germline cysts), which are characteristic for adult ovaries in invertebrates [46], lower vertebrates [66],

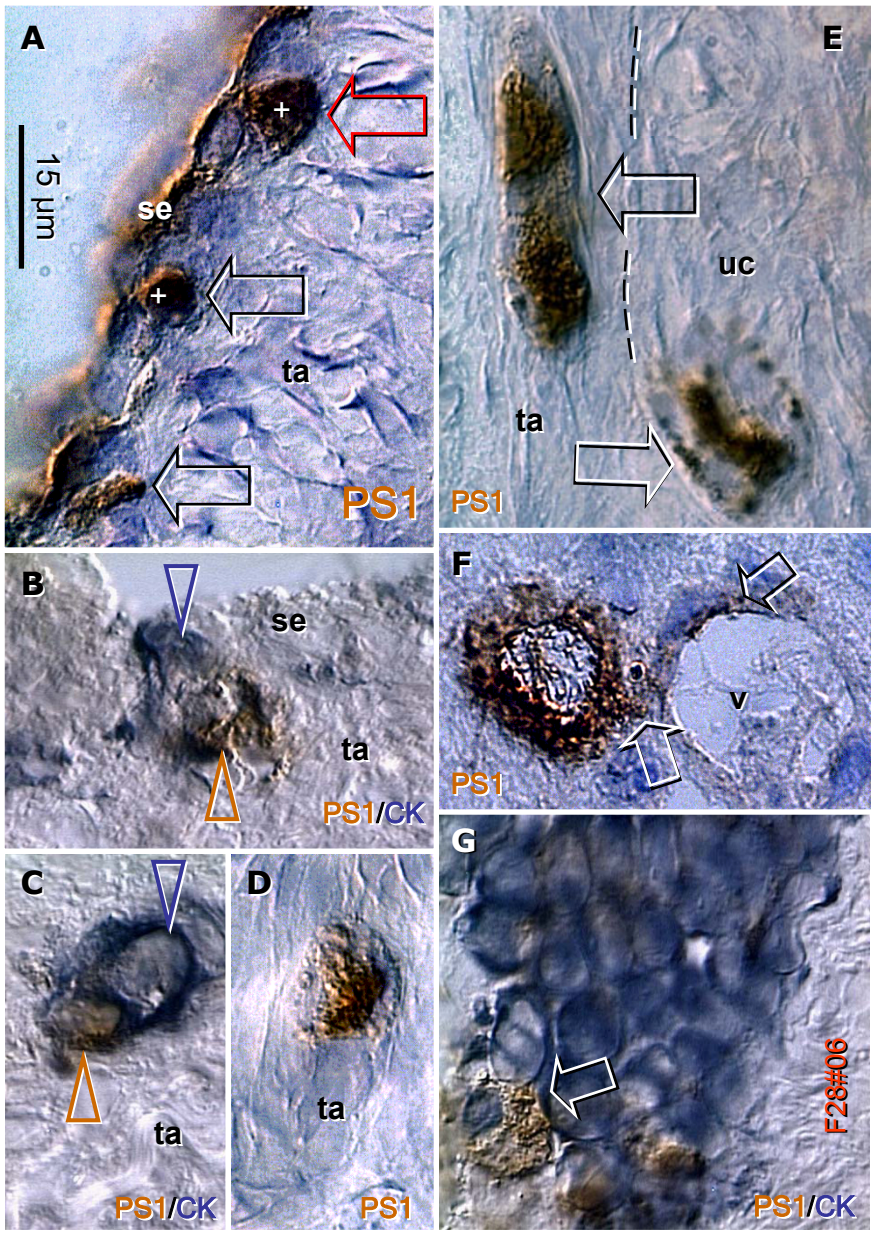

Figure 9

Association of PS1 meiotically expressed oocyte carbohydrate protein with asymmetric division and migration of putative germ cells. A) Segments of SE show cytoplasmic PS1 (brown color) expression (se). Dividing SE cells give rise to cells exhibiting nuclear PS1 immunostaining (+ nuclei, asymmetric division) and descending from the SE (arrows) into tunica albuginea (ta). This is particularly evident in the cell marked with a red arrow. **B**) Except asymmetrically divided SE cell – note CK+ (blue color and arrowhead) and PS1+ (brown color and arrowhead) daughter cells, no PS1 or CK immunoexpression is apparent in this SE segment or in the panel (**C**). **D**) In TA, the putative germ cells increase in size, but nuclear PS1 immunostaining persists. They show a symmetric division (arrow, **E**) and exhibit development of cytoplasmic PS1 immunoexpression when entering the upper (uc) ovarian cortex (white arrow). In the cortex, the cells show diminution of nuclear and increase of cytoplasmic PS1 staining (white arrow, panel **F**), particularly when attached to the cortical vessels (v). In such case, the PS1 immunoexpression appears to be extended toward endothelial cells (black arrow). In some instances, the asymmetric division giving rise to the putative PS1+ (brown color) germ cells could be observed at the periphery of CK+ (blue color) cortical epithelial crypts (arrow, panel **G**). Single (PS1) or double color immunohistochemistry (PS1/CK) as indicated, no hematoxylin counterstain.

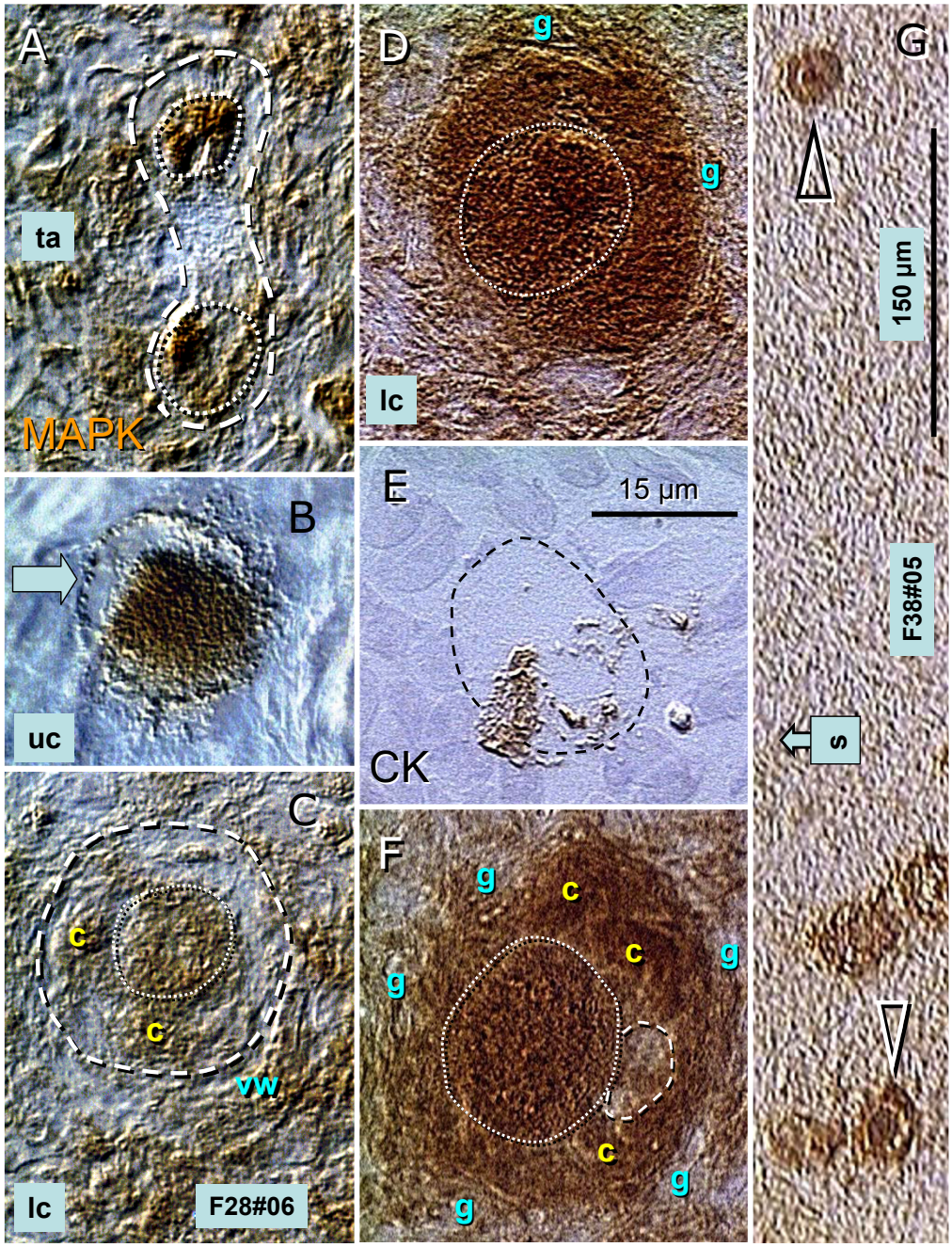

Figure 10

Mitogen-activated protein kinase immunoexpression (brown color) in dividing and differentiating germ cells. Symmetrically dividing putative germ cells dashed line, panel **A**) in the TA (ta) showed strong nuclear MAPK immunostaining dotted lines. The cells showed an increase in size in the upper cortex (uc, panel **B**). Further increase in size of putative germ cells was detected during vascular transport, and accompanied by an appearance of focal cytoplasmic MAPK immunoexpression (c, panel **C**). **D**) During assembly with CK+epithelial nest (see brown color, serial section in panel **E**), the oocytes exhibited strong MAPK immunostaining of both the nuclear (dotted line) and cytoplasmic regions. In freshly formed primary follicles (**F**, see panel **G** for low power magnification of **D** and **F**), the MAPK heavily stained cytoplasmic clusters (c) were apparent, except an isolated paranuclear (Balbiani) body (dashed line). Strong nuclear staining (dotted line) persisted. MAPK (**A-D**, **F** and **G**) and CK single color immunohistochemistry (**G**), with hematoxylin counterstain. "s" arrow in (**G**) points to the distant ovarian surface.

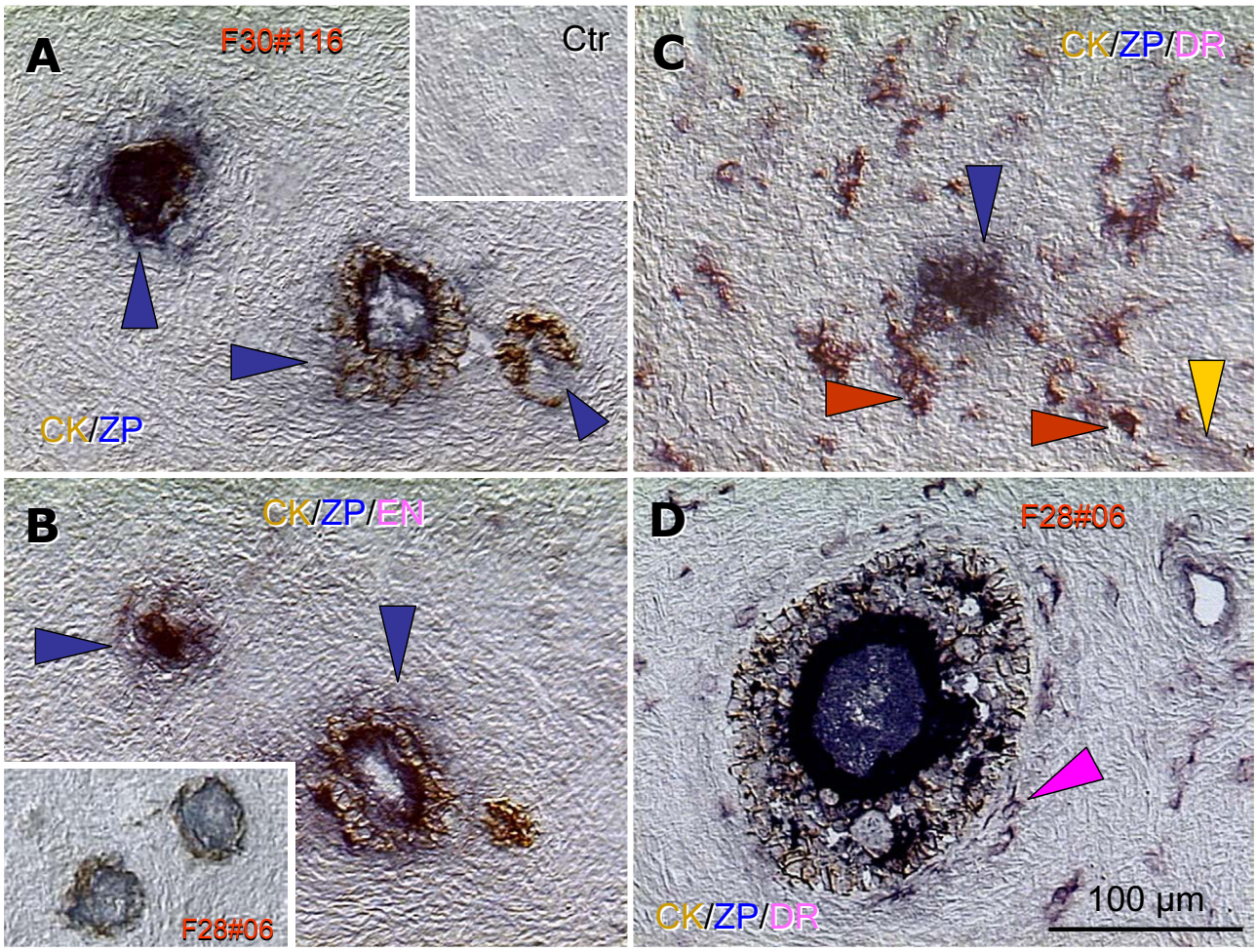

Figure 11
Influx of macrophages during follicular atresia. Double color CK (brown color)/ZP (blue) immunohistochemistry revealed that cohorts of primary and secondary follicles in certain areas of the ovarian cortex showed degenerative changes, characterized in particular by fragmentation of the oocyte structure and dispersion of ZP+ staining among poorly defined layer of granulosa cells and adjacent stroma (arrowheads, panel A; see inset for control immunostaining). Inset in (**B**) shows normal primary follicles in another case. Triple color staining (CK/ZP/DR, panel **C**) revealed numerous large DR+ (purple color) macrophages (red arrowheads) invading the area from adjacent vessels (yellow arrowhead). In contrast, a healthy growing and preantral follicle (panel **D**) shows an association of sporadic small DR+ macrophages with the developing theca (red arrowhead). No hematoxylin counterstain.

and prosimian primates [14-17], and perhaps persist from early periods of life, have been observed in adult human ovaries.

Follicular atresia (Fig. 11)
Degeneration may affect groups of primary (and secondary) follicles, as shown in Fig. 11A,11B,11C. Follicles undergoing atresia show release of ZP staining (blue color) into the neighboring stroma (blue arrowheads, panels A-C). This is associated with an altered oocyte morphology and disorganization of the follicular CK+ (brown) granulosa layer- see center, panel A (inset shows control staining). In addition, there is a considerable influx of large macrophages into the area from the vessels accompanying follicles (purple color, red and yellow arrowheads, panel C). Yet, some investigators have claimed that characteristic morphological features of primary follicle atresia is often difficult to determine

(reviewed in [4]), while others are more confident [54]. In this immunohistochemical study, the assembly of oocytes with epithelial nests was also associated with some release of ZP antigens. However, formation of new follicles was characterized by well defined oocyte nucleus, intraooplasmic CK+ extensions from the nest cell wall, and formation of the Balbiani body, i.e., structures and processes not apparent during follicular regression. Resting normal primary follicles (inset, Fig. 11B) and growing secondary/preantral follicles (panel D) show regular morphology, no leakage of ZP antigens, and only occasional small tissue macrophages associated with the developing theca (arrowhead).

Epithelial crypts – an alternative for germ cell origin (Fig. 12)

Enhanced follicular atresia was accompanied by the appearance of epithelial nests (fragmented epithelial cords) in adjacent segments of the ovarian cortex. Three serial sections show that these nests (left, Fig. 12A,12B,12C) are small CK+ (brown color) spheroidal structures of 20–30 μm in diameter. Also shown is CK+ epithelial crypt (right), likely originating from a deep SE invagination but not communicating with the ovarian surface, as evidenced from serial sections. Arched arrows in panel A indicate a longitudinal arrangement of two stromal bundles, one containing epithelial nests and the other a crypt. The bottoms of these stromal bundles are adjacent (see border lines, panel B) and their migration appears to be influenced by HLA-DR+ (activated [67]) tissue macrophages (purple color, black and white arrows, panel C). An extension from the crypt toward the nest area (yellow arrow) is associated with an accumulation of tissue macrophages (panel C). The red arrow in (B) indicates a weakly CD31+ (purple) adjacent cortical blood vessel.

Panel D shows a more advanced stage of germ cell origin from an epithelial crypt in the lower ovarian cortex of another woman. Note ZP+ staining in the cortex extending from the crypt (blue color, arched arrows). Details are shown in panels E-H, where CK- large round cells (yellow arrowheads) emerge among CK+ (brown) epithelial cells and divide (red arrowheads, panel H). Blue arrowheads (panels E and F) indicate that unstained large round cells are accompanied by ZP+ (blue color) segments, possibly representing an early formation of the germ cell intermediate sections. The dashed line (panel H) indicates the tadpole-shaped cell with the leading nucleus (n), ZP+ intermediate section (is), and a tail (t). The ovarian section from another female (panel I, immunostained as a sample in panel D) shows a lower ovarian cortex with primary follicles in the proximity of an epithelial crypt. Note that the distance between the crypt and follicles (100–150 μm) is similar to that between the crypt and nests in panels A-C. Dashed boxes indicate adjacent CK+ (brown) epithelial nests in the upper ovarian cortex, "s" arrow points toward the ovarian surface.

These observations indicate that adult ovaries exhibiting enhanced atresia of primary (and secondary) follicles initiate formation of new epithelial nests with granulosa cell features [22], one of the prerequisites for the formation of new primary follicles (see Fig. 16 beneath). Cortical crypts, consisting of epithelial cells retaining the relatively embryonic structure of SE cells [22,25], appear to be an alternate source for germ cells. Germ cells entering vasculature may reach epithelial nests at distant destinations, although vascular proximity is not a requirement for follicular development.

An "ovary-within-the ovary" pattern of Thy-1 differentiation protein distribution (Fig. 13)

Why do primary follicles form in the lower ovarian cortex, not just near the origin of their components, primitive granulosa and germ cells? We have reported previously that groups of follicles lie in isolated areas of the cortex, exhibiting an oval arrangement of stromal elements [32]. In the present study, staining for Thy-1 differentiation protein (Thy-1 dp) revealed that groups of primary follicles reside in the center of rounded areas, extending ~400–1200 μm from the ovarian surface, exhibiting virtually no stromal Thy-1 dp immunoexpression, and showing an ovary-within-the ovary pattern (ov-in-ov, Fig. 13). In addition, growth of some follicles in a given cohort is associated with Thy-1 dp+ vasculature (lower vs upper inset). Hence, a lack of Thy-1 dp may be required to maintain primary follicles in the resting state, and the presence of Thy-1 dp may stimulate follicular growth. Note strong Thy-1 immunostaining of the TA fibroblasts (ta, Fig 13).

Oocyte remnants in medullary vessels (Fig. 14)

Another important question is if the number of newly formed follicles is determined by the number of available epithelial nests or the number of generated germ cells. In the first instance, the isolated nests will either persist or degenerate, in the second, the degenerating oocytes not utilized for formation of new primary follicles might be detected.

We utilized double color immunohistochemistry to search for ZP+ (blue color) oocytes not assembled with CK+ (brown) structures. Figure 14A shows a mass of amorphous ZP+ material adjacent to the corpus albicans (CAlb), ZP+ processes and the spread of ZP staining extending into the adjacent stroma (arrow). There are no CK+ structures. A serial section stained as above plus HLA-DR (purple color), a marker of human endothelial cells and tissue macrophages, shows regressing vasculature in the corpus albicans (open arrowhead, panel B). The next serial section (panel C), stained by a control procedure

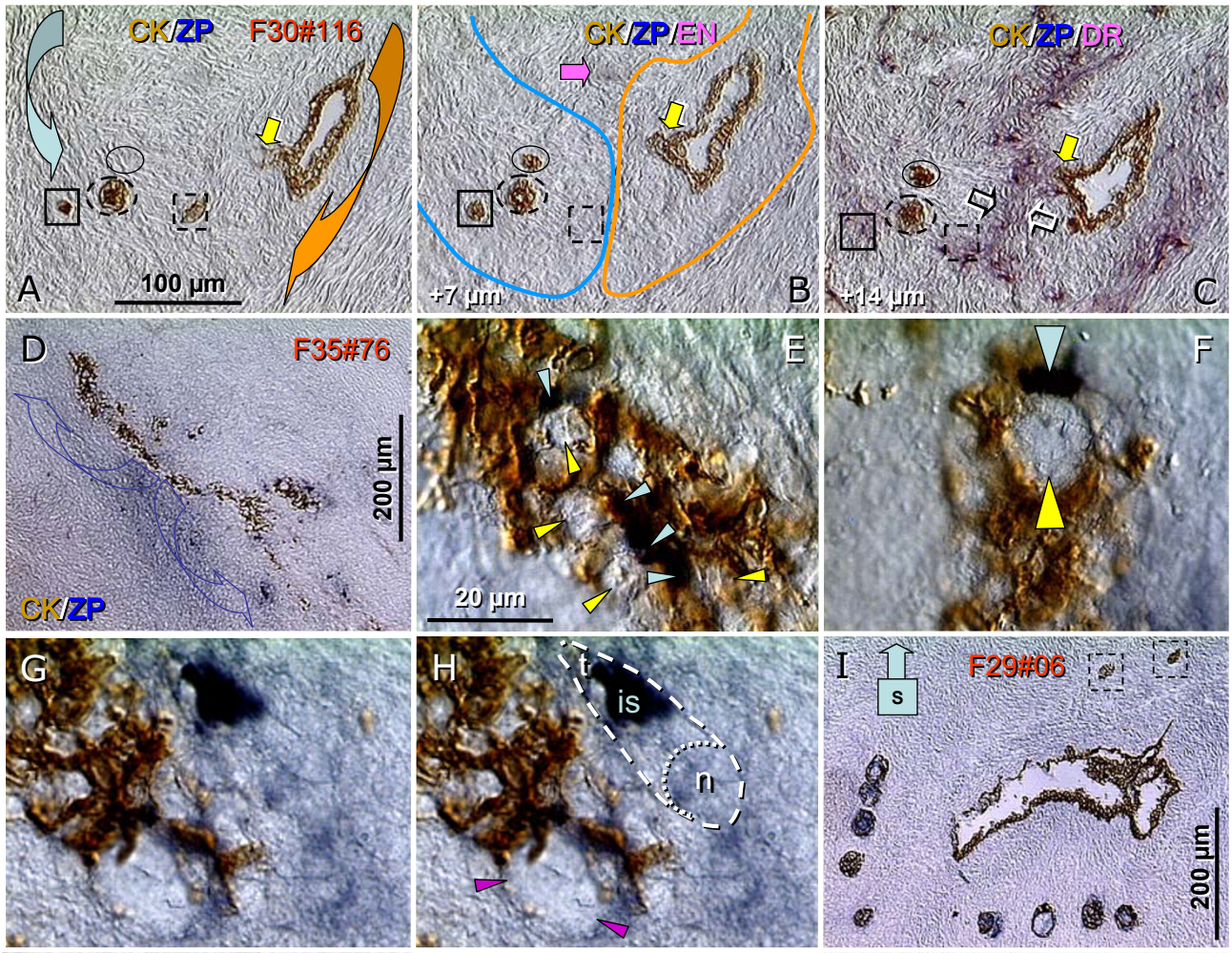

Figure 12

Epithelial crypts – a source of germ cells for the alternative pathway of primary follicle formation. In ovaries showing atresia of follicular cohorts, association of epithelial nests with epithelial crypts has been observed. Panels (**A-C**) show CK+ (brown color) small epithelial nests, as evidenced from serial sections (compare the content of solid and dashed squares and oval areas on the left side). In panel (**B**), weakly CD31+ (purple) adjacent vessel is indicated by a red arrow, solid white arrows in A-C indicate an extension from the crypt toward the nests, and open arrows in (**C**) – see also lines in (**B**), indicate interface between stromal sprouts carrying epithelial nests and the crypt. Panel (**C**) also shows an accumulation of DR+(purple) macrophages around the stromal sprouts, and at their interface in particular. **D**) Remnant of an epithelial crypt (red arrow) from another case shows migration of ZP+ (HSPZ, blue) particles and stromal staining from one side (arched arrow). **E-H**) Details from panel **D** show an appearance of single (yellow arrowheads) and dividing germ-like cells (red arrowheads) among regressing CK+ cells (brown color). Note ZP+ segments (blue color and arrowheads) associated with unstained round cells. Dashed line in (**H**) indicates tadpole-like germ cell with leading nucleus (dotted line), ZP+ (blue color) intermediate section (is), and unstained tail (t). Panel (I) shows an association of primary follicles with the cortical epithelial crypt. Dashed boxes indicate unassembled epithelial nests. Details in text. No hematoxylin counterstain.

(PBS instead of primary antibodies followed by three secondary antibodies and three color substrates plus hematoxylin counterstain of the nuclei), shows that a large vessel is congested with amorphous material (asterisk). Note a lack of staining in adjacent stroma (arrow) except two distant cells (arrowheads) showing brown color, i.e., eosinophils with endogenous peroxidase [68].

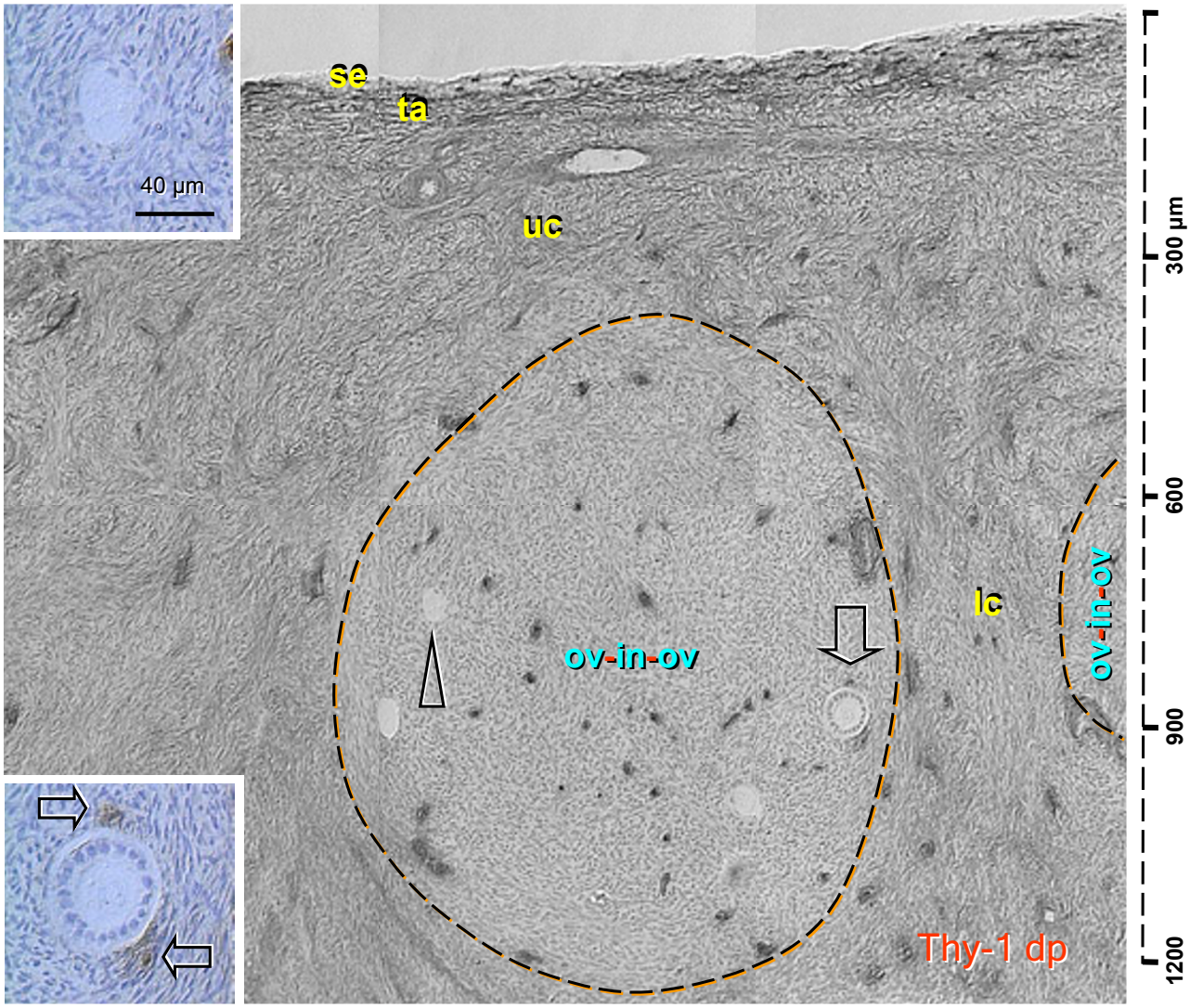

Figure 13
Distribution of Thy-1 differentiation protein in the ovarian cortex – an "ovary within the ovary" pattern. Thy-1 dp was strongly expressed by TA fibroblasts (ta), and moderately in the upper (uc) and lower ovarian cortex (lc) except areas showing an "ovary within the ovary" pattern (ov-in-ov) with virtually no Thy-1 dp immunoexpression except vascular pericytes and smooth muscle cells. These areas characteristically contained primary follicles (arrowhead and upper inset) some of which showed an increase in size accompanied by Thy-1 dp+ pericytes (arrow and lower inset). Hematoxylin counterstain, details in text.

Our observations in ovarian cortical vessels indicate that the vascular pathway of oocytes to their destination (epithelial nests) may be interrupted by vascular degeneration. Figure 14D also shows an accumulation of ZP+ material associated with one of the multiple vessels in the ovarian medulla. Another section from the same ovary (panel E) and another case (panel F) show multiple oocytes accumulated in one of the medullary vessels. Note a lack of CK+ structures, strong ZP cytoplasmic immunoexpression, anchors to the vascular wall and spread of ZP immunostaining to the adjacent stroma (arrow), and a lack of staining in the oocyte nuclei (arrowheads).

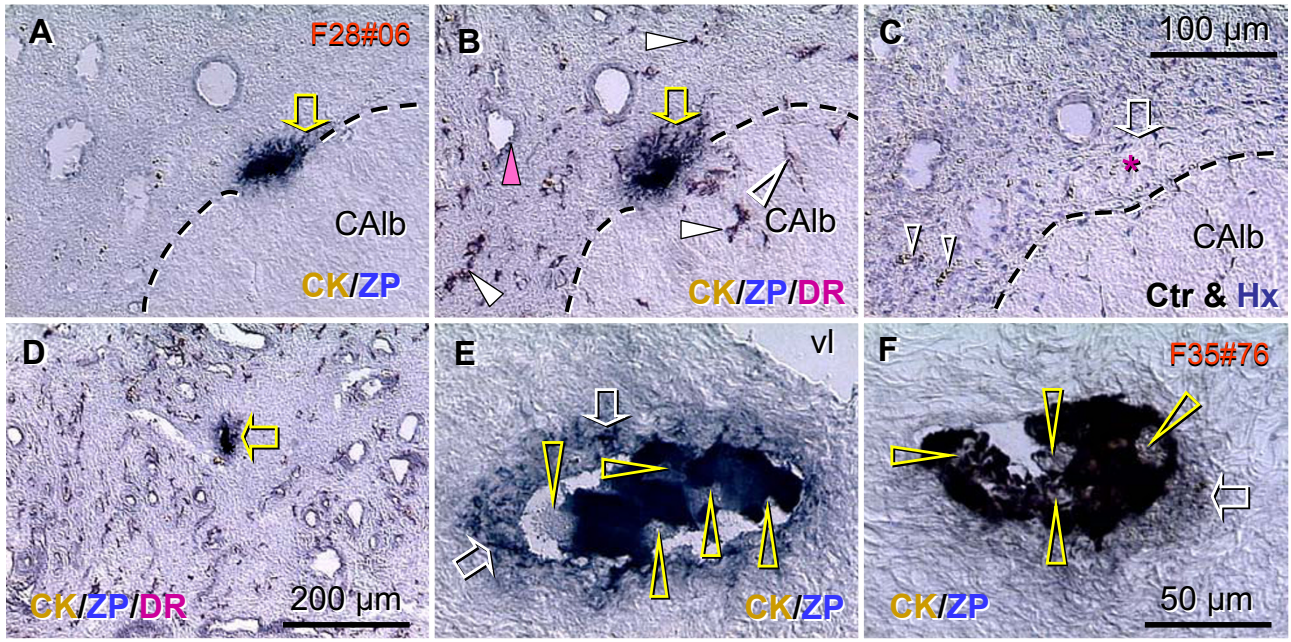

Figure 14

Accumulation of oocytes and their remnants in some medullary vessels. Some medullary vessels showed an embolus-like accumulation of ZP+ (HSPZ, blue color) material, either at the structures showing vascular regression, e.g., corpus albicans (CAlb, panels **A-C**), or without apparent vascular regression (panel **D**). In some instances, a higher magnification revealed the presence of multiple unstained oocyte nuclei (arrowheads, panels **E** and **F**). No hematoxylin counterstain except control staining in panel (C). vl, adjacent vascular lumen. Further details in text.

An accumulation of oocytes in some ovarian medullary vessels was observed in four of twelve cases studied (33%). This suggests that the differentiation of oocytes during the reproductive period is a relatively frequent event. These ovarian samples showed preparation or ongoing formation of new primary follicles. When detected, accumulation of oocytes in some medullary vessels was present in the samples from both ovaries. Yet, there were eight cases showing no such activity. These ovaries rarely showed primary follicles in the ovarian cortex. This agrees with observations of Block [53], who observed a similarity between the numbers in the right and left ovaries but wide individual variation between cases during the optimal reproductive period. Our observations suggest that the formation of new primary follicles is not a permanent but transient process, which may occur during certain period of the ovarian cycle. This idea was proposed by Edgar Allen [69] and Evans and Swezy [70]. Although we did not investigate a large number of patients, our observations indicate that new primary follicles are likely to be formed during the late luteal phase, as evidenced from the patient's history, ovarian (CL) immunohistochemistry, and endometrium morphology.

Follicle numbers in human ovaries (Fig. 15)

We performed statistical analysis (one way analysis of variance and post-hoc test) of the Block's (including ovaries from neonatal, premenarcheal, and young-adult females) [53,63,64] and Gougeon's (mostly premenopausal females) data [54] on the variation of the number of human ovarian primary follicles at different ages, between the birth and 50 years of age. Figure 15A shows that, when compared to neonatal ovaries, the first significant decline occurs in the age group of 18–24 years. No significant change is apparent during the 20 year optimal reproductive period, between 18 and 38 ± 4.1 SD years. However, age groups 40–44 and 45–50 show significantly lower numbers compared to other age groups. Details on descriptive statistics are provided in Fig. 16B. Note that the mean and maximum values (highlighted) show a plateau between 0–16, 18–38 and 40–50 years of age.

Discussion

We report that mesenchymal cells in human ovarian TA are capable of expressing CK and differentiate into SE cells by a mesenchymal-epithelial transition *in vivo*. Through this transition, the bipotent mesenchymal cells in TA give

A

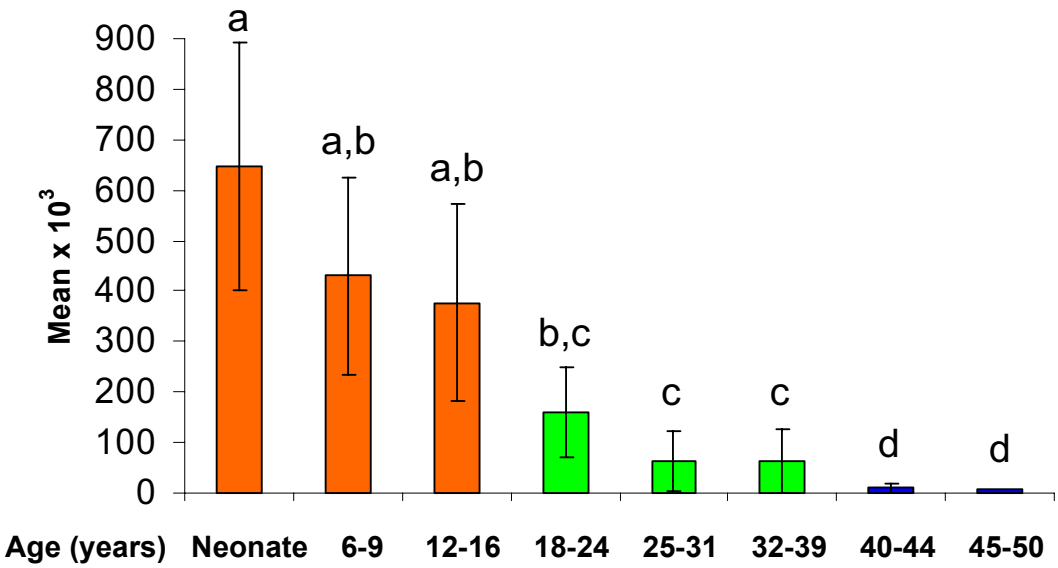

B

x 1000	*Neonate*	*6-9 y*	*12-16 y*	*18-24 y*	*25-31 y*	*32-38 y*	*40-44 y*	*46-50 y*
Mean	648.7	430.1	376.2	158.9	62.1	63.0	9.6	6.1
SD	245.4	205.5	195.5	83.7	55.1	49.3	9.9	8.0
Minimum	352.0	85.0	85.0	39.0	8.1	15.0	0.4	0.6
Maximum	**1126.0**	**755.0**	**591.0**	**290.0**	**228.0**	**208.0**	**28.3**	**39.3**
Sum	6487.0	4301.0	1881.0	1271.0	807.3	945.7	153.2	140.3
Count	10.0	10.0	5.0	8.0	13.0	15.0	16.0	23.0
Conf (95%)	175.5	147.0	242.7	70.0	33.3	27.3	5.3	3.5

Figure 15

Age-related changes in primary follicle numbers in both human ovaries (A) and descriptive statistics (B). A) Statistical analysis of transformed cumulative data [Y = Log(Y)] reported by Block [53,63,64] and Gougeon [54] shows P < 0.0001 for one-way ANOVA. Tukey-Kramer Multiple Comparison post-test revealed that compared to neonatal ovaries a significant difference in follicle number first appears in the age group of 18 to 24 years. However, no significant difference was observed during the 20 years of optimal reproductive period, between females 18–38 years of age. Yet, the ovaries obtained from 40–50 year old females showed a significantly lower number of primary follicles vs. all other age groups. **B**) Descriptive statistics indicates plateau of the maximum follicle numbers (highlighted) during the 6–16, 18–38, and 40–50 age periods, associated with a lack of statistical significance between mean values ± SD – see panel (**A**).

rise to: (1) nests of primitive granulosa cells in the ovarian cortex, and (2) primitive germ cells which differentiate into oocytes and assemble with granulosa cell nests to form new primary follicles. Hence, TA mesenchymal cells represent a progenitor cell with a commitment to either of two distinct terminally differentiated cell types.

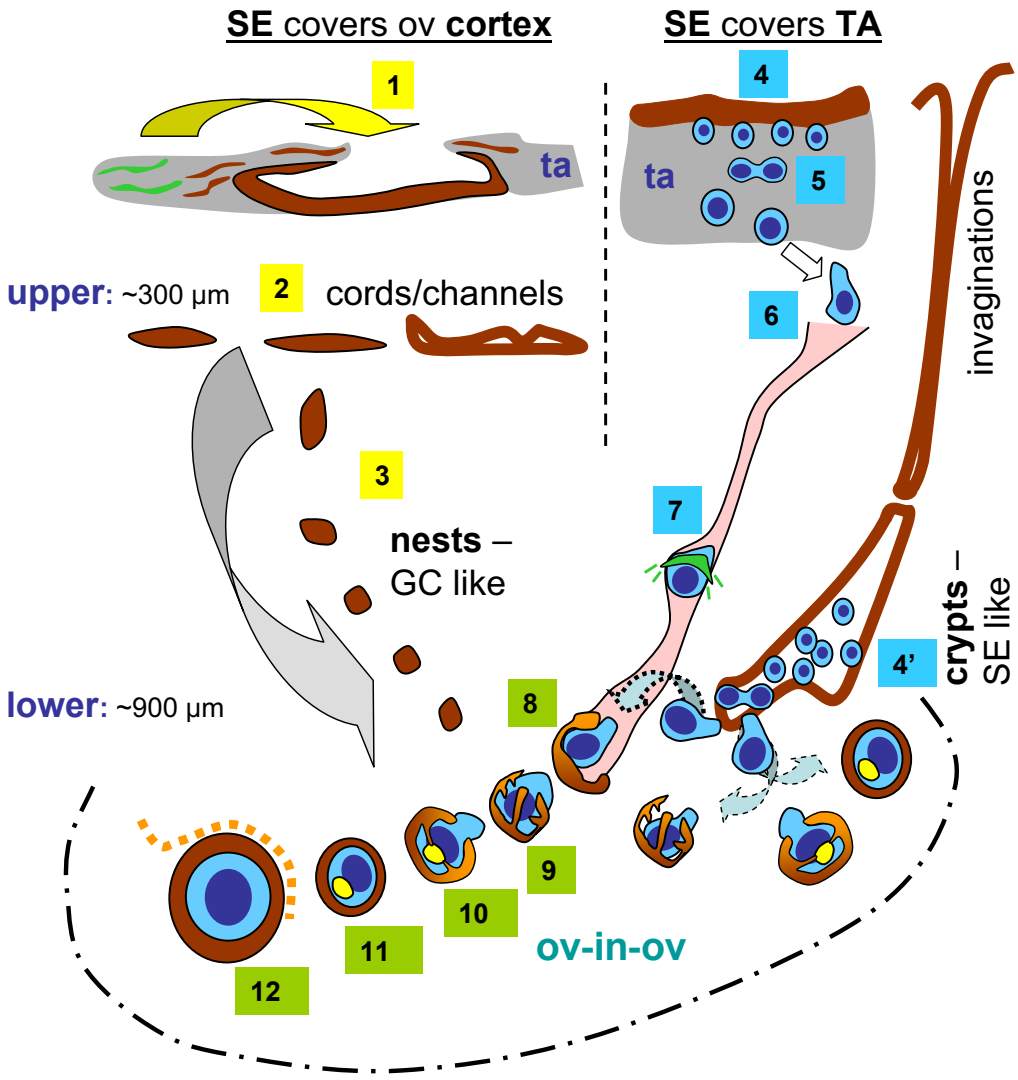

Figure 16

Working model of possible pathways for formation of primary follicles in adult human ovaries (updated from Ref. [32]). **1**) Ovarian tunica albuginea (ta) stem cells (green color) differentiate into the CK+ fibroblasts (red color) and by mesenchymal-epithelial transition give rise to the SE cells directly covering the ovarian cortex (arched arrow). **2**) Closing of TA flaps (see Fig. 1) results in the formation of epithelial cords/channels in the upper ovarian cortex (see Fig. 3). Fragmented epithelial cords give rise to the epithelial nests, which resemble primitive granulosa cells [22] and descend into the lower ovarian cortex. **4**) Depending on certain in situ (stromal) influences, the TA progenitors differentiate into the SE cells covering TA, which may, by asymmetric division, give rise to the ZP+ germ cells. **5**) These putative germ cells may symmetrically divide, descend into the ovarian cortex, and associate with adjacent cortical vessels (**6**). Intravascular transport (**7**) is associated with a substantial increase of germ cell size and with development of ZP+ anchors (green lines), which may serve to slow down the transport speed and signal the epithelial nests to associate with a particular vascular segment. **8**) The intravascular germ cells differentiating into the oocytes are picked up by epithelial nests associated with the proper cortical vessels. Such oocyte-nest complexes show an "octopus-like" (**9**) formations during the early stage of assembly, and a formation of the Balbiani body during the intermediate stage (yellow body, **10**). The Balbiani body persists in resting primary follicles (**11**), but diminishes upon the growth promoting signals, including Thy-1 dp signaling derived from the follicle-accompanying vessels (**12**, dashed line). An alternative pathway for the germ cell origin from TA precursors (**4**') consists of a constitution of cortical crypts formed by SE-like embryonal type cells [22,25], possibly originating from, but not necessarily connected with, the deep SE invaginations, as evidenced from serial sections. The "alternative" pathway of germ cell origin may supply the oocytes directly to the neighboring nests (dashed arched arrows) and, via vascular transport (dotted arched arrow), saturate distant nests to form the primary follicles.

Mesenchymal-epithelial and epithelial-mesenchymal transitions

Multipotential progenitor cells exhibiting a mesenchymal phenotype and capable of differentiation into distinct cell types have been derived from various other adult tissues [71-75]. Mesenchymal-epithelial and epithelial-mesenchymal transitions may reflect a plasticity of progenitor cells in a particular microenvironment. They may occur sequentially (mesenchymal-epithelial followed by epithelial-mesenchymal transitions) under the influence of the extracellular matrix, cytokines (transforming growth factor β, fibroblast growth factor, hepatocyte growth factor, epidermal growth factor, BMP2 and BMP4), adhesion molecules (integrins, E-cadherins), membrane receptors, intercellular junctions, signaling pathways (MAPK) or transcription factors β-catenin) commonly produced in the embryo and less frequently in adult organisms. Such transitions are examples of manifestations of cell plasticity and subsequent dramatic changes resulting in lineage commitments into certain cell types (reviewed in [65]).

Many cytokines and morphoregulatory molecules are produced by specific stromal elements – fibroblasts/pericytes, macrophages and T lymphocytes, which are involved in mesenchymal-epithelial transitions [76-82] and stimulate differentiation of epithelial cells (reviewed in [83]). We have earlier demonstrated that such cells accompany appearance and migration of germ-like cells in adult human ovaries, and suggested that age-induced diminution of immune system function (immune senescence) may cause a diminution of follicular renewal [32].

Hypothesis

Having in mind these exciting findings, we speculate that the development of TA in perinatal human ovaries [19,20] is a result of an epithelial-mesenchymal transition of coelomic ovarian SE cells. During adulthood, the mesenchymal cells in TA undergo a mesenchymal-epithelial transition back into ovarian SE cells with an embryonic character [25]. These cells still have the ability to become granulosa or germ cells, probably depending on the influences of neighboring stromal cells (microenvironment). However, a differentiation of germ cells from SE cells, which originate from TA mesenchymal precursors, appears to represent a novel three step transition, i.e., mesenchymal > epithelial > germ cell transition. When the presumptive perinatal transition is included, the four step transition can be determined: Epithelial (fetal SE) > mesenchymal (perinatal development of TA) > epithelial (adult SE and granulosa cells) > germ cells.

A schematic view of possible pathways for formation of primary follicles from TA mesenchymal precursors in adult human ovaries is shown in Fig. 16. The process is initiated by the differentiation of CK- to CK+ mesenchymal cells in TA. These CK+ mesenchymal cells are associated with TA flaps and give rise to SE cells directly covering the ovarian stroma (yellow arched arrow, step 1). The closing of TA flaps results in the formation of bilaminar epithelial channels and solid cords in the upper ovarian cortex (2). These cords are fragmented into epithelial nests (granulosa cell-like cells [22]), which descend by stromal rearrangement into an area in the lower cortex exhibiting lack of Thy-1 dp expression and having an "ovary within the ovary" (ov-in-ov) pattern (3).

Mesenchymal cells expressing CK also differentiate into SE cells covering the TA. These cells can be stimulated to give rise to the ZP+ primitive germ cells (asymmetric division), which descend into the TA (4). Then they divide symmetrically (5) and enter the upper ovarian cortex and adjacent cortical vessels (6). During vascular transport (7), the germ cells extend ZP+ projections (green lines) to the vascular wall, which may delay their transport and enable maturation into the oocytes. Intravascular oocytes are picked up by epithelial nests (8), and this results in the formation of new primary follicles (9). An "alternative" pathway for germ cell origin (4'), which may exist along with the "classical" pathway, consists of germ cell differentiation from epithelial crypts in the ovarian cortex (SE-like cells [22]), which may originate from deep SE invaginations. This "alternative" pathway can supply germ cells to the neighboring nests directly (dashed arched arrows), or through the vascular transport (dotted arched arrow) to nests at distant destinations.

During follicle formation, nest cells contribute to the development of the Balbiani body (10), which contains all the mitochondria of the oocytes and persists in resting human primary follicles (11) [45]. Interestingly, the Balbiani body strongly expressed CK18, but was virtually undetectable with the antibody against other cytokeratins expressed by granulosa cells (CK 5, 6, 8, 17). This observation suggests that CK18 might be specific for granulosa cell mitochondria supplied to oocytes in human ovaries. Upon certain signals, such as Thy-1 dp secreted by vascular pericytes (dashed curve), the mitochondria are released from the Balbiani body, and the oocyte and follicle enter a stage of progressive growth (12).

Mammalian female gametogenesis and evolution

From a phylogenetic viewpoint, it seems contradictory that mammalian females, including humans, would evolve a uniquely retrogressive reproductive mechanism, whereby they are required to preserve their gametes from the fetal period for up to several decades. Since mammalian female germ cells differentiate from somatic lineage, why would human female gametes and primary follicles differentiate during the fetal period, if they are not needed

until puberty several years later? Development of the immune tolerance toward self during fetal period of life [67] might explain this early differentiation of germ cells and primary ovarian follicles. We have earlier suggested that germ cells and oocytes differentiate in fetal ovaries in order to be recognized as self structures [55]. If this does not occur, the oocytes and primary follicles may face the fate of the corpus luteum, which is absent in fetal ovaries and whose functional life in the adult ovary, except during the immunologically unique situation of pregnancy, lasts for only several days.

Germ cells and oocytes in the ovarian surface epithelium

Do female germ cells in fetal ovaries migrate from the ovarian stroma to the SE and leave the ovary? This process has been suggested to contribute to a reduction of the germ cell and oocyte pool in fetal and neonatal ovaries [19,84,85]. There are two critical issues to be discussed regarding these views.

Firstly, the size of germ cells in the fetal SE (10 μm) is substantially smaller than that of germ cells and oogonia in the adjacent cortex (15–20 μm). Secondly, like in tadpole or sperm, the germ cell migration is always guided by a bigger proportion of the cell (nuclear region) with the tail segment being the last. Yet, some images presented in Ref. [19,84] and our recent observations [56] indicate that germ cells with amoeboid evaginations in the SE of fetal ovaries show an orientation of the nucleus toward the ovarian stroma. In addition, we show that in adult ovaries, the ZP+ germ cells originate from the SE and enter the ovarian stroma. Yet, we have reported previously that large cells resembling oocytes may be detected in the SE and, like in term human fetuses [85], apparently are extruded in women over 40 years of age [32].

It appears that 10 μm ZP+ germ cells originate via asymmetric division of SE cells (Fig. 9A,9B,9C). If needed – such as in the second trimester of intrauterine life and the optimal reproductive period, germ cells are stimulated to descend into the ovarian stroma and contribute to the formation of new primary follicles (Fig. 10). Otherwise, germ cells may be prevented from entering the ovarian stroma, thereby left to differentiate within SE into oocytes, and stimulated to leave the ovary. One may speculate that since the Balbiani body (source of mitochondria) can not be formed without the contribution of granulosa cells, such oocytes have no chance to mature functionally, complete the first meiotic division, and be fertilized.

Presumptive germline stem cells were recently reported to reside in the SE of mouse ovaries (63 ± 8 cells per juvenile ovary, n = 4 mice) [13]. The ovoid cells demonstrated are unusually large (~30–40 μm in diameter). In reality, however, such large presumptive germline stem cells, and their protrusion from the ovarian surface toward bursal cavity, as shown by Johnson et al. in Fig. 2a[13], closely resemble those seen with an extrusion of large oocytes from the ovary, which has been described in neonatal human ovaries [85], or in ovaries of premenopausal women [32] (see also above).

Differentiation of germ cells and MAPK expression

The resting primary follicles have been shown to exhibit strong cytoplasmic but no nuclear immunoexpression of MAPK [31], an enzyme which stimulates the differentiation of somatic and germ cells [86,87]. We show that both the cytoplasmic and nuclear MAPK staining is apparent during oocyte assembly with epithelial nest cells, as well as in actually formed (adjacent) primary follicles. Interestingly, the paranuclear Balbiani body in primary follicles showed a low MAPK immunoexpression, suggesting a lack of its activation after follicle formation. Translocation of cytoplasmic to nuclear MAPK expression appeared with an increase of follicle size (initiation of follicular growth), but MAPK staining was virtually absent in oocytes of primary follicles undergoing atresia [31].

These data indicate that differentiation of germ cells, oocyte assembly with nests of primitive granulosa cells, and oocyte growth in secondary follicles requires the nuclear expression of MAPK. A lack of nuclear MAPK expression is associated with oocytes in resting primary follicles. On the other hand, cytoplasmic MAPK expression appears during the differentiation of germ cells into oocytes. It persists in oocytes of resting follicles, and is depleted in the oocytes undergoing atresia. This indicates that cytoplasmic MAPK expression in resting (healthy) follicles may represent a readiness of oocytes for the nuclear transfer required for resumption of oocyte (follicular) growth. Also, characteristics of MAPK immunoexpression appear to be excellent indicators of the follicular condition – follicle formation, resting vs. degenerating primary follicles, and resumption of follicular growth.

Alternative pathway for germ cell origin in adult human ovaries

This study may contribute to a better understanding of the mechanisms enabling mammalian females to maintain a relatively constant number of primary follicles during the optimal reproductive period, despite the continuous depletion of primary follicles through atresia. In our previous report [32], we described the occurrence of putative germ cells in the surface epithelium covering the tunica albuginea – a "classical" pathway of germ cell origin suggested by Waldeyer [1]. The data presented here indicate that an "alternative" pathway also exists, consisting of germ cell development from epithelial crypts in the ovarian cortex.

We show that in the ovarian cortex, the crypts lie in the proximity of epithelial nests (fragmented cords), and the same applies for some primary follicles. It is possible that this "alternative" pathway occurs more regularly during the reproductive period of life than the "classical" pathway characteristic for human fetal ovaries, because crypts reaching the lower ovarian cortex can deliver germ cells to the neighboring epithelial nests directly, without requiring vascular delivery. Furthermore, it appears that the germ cells are capable of reaching epithelial nests by their own movement, up to a distance of about 150 μm (Fig. 12). However, vascular transport of germ cells may still occur for nests which are more distant.

The "ovary within the ovary" pattern

Primary follicles are typically located in isolated segments of the ovarian cortex, which exhibit a lack of Thy-1 dp expression by cortical fibroblasts. Production of Thy-1 dp, a primitive member of the immunoglobulin gene superfamily of molecules [88], by vascular pericytes is not only associated with a progression of follicular growth [32,89], but with differentiation of epithelial cells in general [83]. We show that growing follicles in the "ovary within the ovary" segments are accompanied by Thy-1 dp secretion from vascular pericytes, in contrast to the lack of vascular activity associated with resting primary follicles (Fig. 13). It has been suggested that the number of follicles entering growth from a given cohort is under the control of Thy-1 dp secretion from vascular pericytes [32], possibly regulated by the autonomic ovarian innervation, which is involved in the regulation of quantitative aspects of tissue homeostasis [89,90]. Consequently, preservation of primary follicles in the resting state appears to require lack Thy-1 dp stromal expression.

Vascular transport

To reach distant destinations during embryonal period of life, germ cells in large mammals have been shown to utilize a vascular route [4,42], and a similar mechanism may operate in adult human ovaries [32]. It remains unclear, however, why cells leave the circulating blood at a certain site. We show that germ cells can be detected within and around the cortical vessels of adult human ovaries. During vascular transport, germ cells increase in size and show ZP+ projections toward the vascular wall. These ZP+ projections may be a signal for epithelial nests (primitive granulosa cells) to associate with the particular vessel involved in the oocyte transport. Blood transport is rapid, so one may wonder that this can be done within few seconds or less.

We propose that the ZP+ projections from intravascular germ cells/oocytes represent anchors to the vascular wall, which may substantially prolong the time in which the cells are transported toward their targets. Also, association of epithelial nest with the vascular wall in the lower ovarian cortex appears to result in the formation of a pocket at the vascular side (Fig. 7A,7B,7C,7D, 8C), enabling blood flow to pass uninterrupted and bring the slowly mowing oocyte. The association of epithelial nests with a particular vascular segment may explain the often observed close (side by side) association of primary follicles in adult human ovaries (see Fig. 3,5,8 and ref. [48]). In addition, epithelial nests are either in contact or penetrated by nerve terminals [22]. Neural signaling may contribute to their association with proper vessels. Local involvement of tissue macrophages may play a role, at least in some instances (see Fig. 12), and their function may decline with age advancement [32,91-94]. Finally, in spite of their effort, intravascular oocytes may not succeed in their attempt to associate with epithelial nests. This may be due to the limited number of nests produced in a given time and the regression of the blood flow, e.g., through the corpus albicans (Fig. 14A,14B,14C). Unused oocytes leave the medullary vessels (Fig. 14D) or anchor to the vascular wall and degenerate (Fig. 14E,14F).

Oocyte remnants

We speculate that each germ cell emerging in adult ovaries has a limited period of time during which it must assemble with epithelial nests and form the Balbiani body in order to persist. Each primitive germ cell will differentiate into the oocyte during a certain period of time, regardless if it is utilized for primary follicle formation or not. An exciting aspect of this report is the occurrence of accumulated oocytes and oocyte remnants in some medullary vessels. Their detection may document an ongoing differentiation of new oocytes, since these oocyte remnants have been observed only in ovaries exhibiting the formation of new primary follicles. It is believed that the total number of oocytes produced within a given time in adult ovaries exceeds by several fold the number of oocytes successfully forming primary follicles. This indicates that the number of newly formed primary follicles is determined by the number of available epithelial nests. Since the nests of primitive granulosa cells are innervated [22], and autonomic innervation determines quantitative aspects of tissue homeostasis [32,89,90], the number of newly formed primary follicles (adaptive folliculogenesis) could be under the neural control. Our unpublished observations indicate that there are no such oocyte remnants in women >40 years of age. This is in a good agreement with the significant decline of the follicular pool reported by others [53,54].

Follicular atresia

Atresia of primary follicles is common during the reproductive period of human females [51]. Our observations suggest that it is a rapid process, assisted by the massive influx of macrophages. The process resembles immune-

system mediated corpus luteum regression [94]. Gougeon suggested that depletion of the primary follicle pool is caused mainly by atresia in younger women and by entrance into the growing pool in older women, with the change-over at 38 ± 2.4 years [54]. Since cyclic ovarian function continues in "early premenopausal" women, we speculate that ~10000 primary follicles detected during the age period 40–44 years (Fig. 15B) is a sufficient depot for continuation of ovulatory ovarian function. A 50000 difference compared to younger females fits well with the observation that 70–95% of oocytes in primary follicles show various stages of degeneration [51,52]. It appears that Gougeon was right, and it is possible to conclude that the pool of healthy primary follicles is at least 10000 during the reproductive years.

In younger females, an ongoing atresia of primary follicles appears to be associated with preparation for a new wave of follicular formation. We propose that during the optimal reproductive period in human females, ongoing atresia affects groups of older primary follicles, and this is compensated for by formation of new primary follicle cohorts. Such follicular turnover may prevent an accumulation of spontaneous or environmentally induced genetic alterations of oocytes in resting primary follicles.

Environmental hazards are increasing, and they include pollutant emissions, radiation, nutrition containing dangerous chemicals, synthetic fertilizers and toxic pesticides, and (retro)viral diseases. In addition, human population is also compromised by pharmaceutical and addictive drugs, alcohol consumption and smoking, and cytostatic and radiation therapy. Renewal of healthy oocytes is apparent from former report of the Scientific Committee of United Nations indicating that women, which were subjected to the sterilizing dose of radiation from atomic bombs in Hiroshima and Nagasaki, eventually resumed menstrual cycles, and some of them gave a birth to healthy babies [95]. This indicates that human females, and possibly some other mammalian species, may have evolved a sophisticated mechanism for follicular renewal resisting environmental threats, contrasting a persistence of (potentially vulnerable) germline stem cells in adult ovaries of other species, e.g., Amphibia [66].

The atresia and renewal of the existing follicular pool may gradually diminish by the end of the third decade of life, and remaining primary follicles may persist without replacement. Since some primary follicles can still be detected in ovaries of females at the end of the fourth decade of life (blue columns, Fig. 15), and such follicular pool in essence declines during the fourth decade of life by transformation into the growing follicles [54], it is possible that in ovaries of human females, primary follicles persist for up to 12–14 years.

However, it is well documented that advanced maternal age is often associated with compromised oocyte quality, aneuploid embryos, and higher rate of Down syndrome, anencephaly, and multiple fetal congenital anomalies resulting from abnormal chromosomes 13, 16, 18, 21, 22, X, and Y [96-112], mainly due to the non-disjunction during oocyte meiosis [97].

The frequency of abnormal fetal karyotypes in different maternal age groups was found to increase from 1:20 at 38–40 years, to 1:16 at 41–43 years, and finally to 1:4.5 in women of 44–46 years [96]. Similar data were reported in another study, where 2 of 123 cases in 35- to 39-year-old women showed an incidence of chromosomal anomalies as high as 1.6%; 7 of 117 cases in 40- to 44-year-old mothers an incidence of 6.0%; and 4 of 16 mothers in the 45- to 49-year-old age group an incidence of 25.0% [97]. Also, the rate of all clinically significant chromosomal abnormalities of cytogenetically abnormal fetuses considered together was about five per 1,000 at age 35 years, 15 per 1,000 at age 40 years, and 50 per 1,000 at age 45 years [98].

These data indicate that the longer resting primary follicles persist within the ovary, the lower is the capacity of oocytes to produce normal human progeny. Interestingly, 12–14 year life span of primary follicles also coincides with the human female age at menarche, and one may speculate that fetal primary follicles may persist (orange columns, Fig 15) till the beginning of regular ovarian function, when an initiation of folliculogenesis (formation of new primary follicles) resumes and lasts during the optimal reproductive years (green columns, Fig 15).

Conclusion

This study expands our earlier and recent observations and views on the formation of germ cells in adult human ovaries [31,32,55,56]. Earlier and recent *in vivo* and *in vitro* studies have shown that mouse embryonic germ cells differentiate from somatic lineage [7-9,11,12] and adult ovaries of prosimian primates and mice possess mitotically active germ cells [13-17] of uncertain origin. We provide direct evidence that in ovaries of adult human females, the components for new human primary follicles, primitive granulosa and germ cells, differentiate sequentially and *de novo* from the CK+ mesenchymal progenitor cells residing in the ovarian tunica albuginea, and new primary follicles are formed by assembly of oocytes with nests of primitive granulosa cells in the ovarian cortex. In contrast to males, adult human female gonads do not possess germline stem cells. This also contrasts with a continuous preservation of the germline stem cells in ovaries of invertebrates, lower vertebrates, birds, prosimian primates, and possibly mice. The number of newly formed primary follicles in adult human ovaries appears to be determined by the number

of developing nests of primitive granulosa cells supplied by a higher number of available oocytes. Formation of new primary follicles throughout the reproductive period may compensate for the well documented atresia of a significant proportion of the follicular pool. This may contribute to the selection of the best possible oocytes and ensure preservation of the relatively constant number of primary follicles found in human females between 18 and 38 years of life. Differentiation of primitive granulosa and germ cells from the bipotent mesenchymal cell precursors of TA in adult human ovaries, and by extrapolation in some other mammals with reproductive period distant from fetal folliculogenesis, may represent a most sophisticated mechanism created during the evolution of female reproduction. It appears that during the reproductive period in human females, the pool of primary follicles does not represent a static but a dynamic population of differentiating and regressing structures. An essential mission of such follicular turnover might be elimination of spontaneous or environmentally induced genetic alterations of oocytes in resting primary follicles.

Acknowledgments

The authors wish to thank anonymous reviewers for constructive criticism and valuable comments. Kind donations of HSPZ, HSRZ and PS1 antibodies by Dr. Bonnie S. Dunbar of the Department of Molecular and Cellular Biology, Baylor College of Medicine, Houston, Texas, USA; HSPZ antibody by Dr. Satish K. Gupta of the National Institute of Immunology, New Delhi, India; HLA-DR antibody by Drs. Ivan Hilgert and Vaclav Horejsi of the Institute of Molecular Genetics, Academy of Sciences of the Czech Republic, and Faculty of Sciences, Charles University, Prague, Czech Republic; human Thy-1 dp antibody by Dr. Rosemarie Dalchau of the Institute of Child Health, University of London, London, UK; and swine anti-mouse IgG peroxidase conjugate by Dr. Jana Peknicova of the Department of Biology and Biochemistry of Fertilization, Institute of Molecular Genetics, Academy of Sciences of the Czech Republic, Prague, Czech Republic, are gratefully acknowledged.

References

1. Waldeyer W: *Eierstock und Ei. Leipzig: Engelmann* 1870.
2. Weissmann A: *Die Continuitat des Keimplasmasals Grundlage einer Theorie der Vererbung* Jena: Fischer-Verlag; 1885.
3. Franchi LL, Mandl AM, Zuckerman S: **The development of the ovary and the process of oogenesis.** In *The Ovary* Edited by: Zuckerman S. London: Academic Press; 1962:1-88.
4. Baker TG: **Oogenesis and ovarian development.** In *Reproductive Biology* Edited by: Balin H, Glasser S. Amsterdam: Excerpta Medica; 1972:398-437.
5. McLaren A: **Signaling for germ cells.** *Genes Dev* 1999, **13:**373-376.
6. Kelly SJ: **Studies of the developmental potential of 4- and 8-cell stage mouse blastomeres.** *J Exp Zool* 1977, **200:**365-376.
7. Ginsburg M, Snow MH, McLaren A: **Primordial germ cells in the mouse embryo during gastrulation.** *Development* 1990, **110:**521-528.
8. Lawson KA, Hage WJ: **Clonal analysis of the origin of primordial germ cells in the mouse.** *Ciba Found Symp* 1994, **182:**68-84.
9. Tarn PP, Zhou SX: **The allocation of epiblast cells to ectodermal and germ-line lineages is influenced by the position of the cells in the gastrulating mouse embryo.** *Dev Biol* 1996, **178:**124-132.
10. Lawson KA, Dunn NR, Roelen BA, Zeinstra LM, Davis AM, Wright CV, Korving JP, Hogan BL: **Bmp4 is required for the generation of primordial germ cells in the mouse embryo.** *Genes Dev* 1999, **13:**424-436.
11. Hubner K, Fuhrmann G, Christenson LK, Kehler J, Reinbold R, De La FR, Wood J, Strauss JF III, Boiani M, Scholer HR: **Derivation of oocytes from mouse embryonic stem cells.** *Science* 2003, **300:**1251-1256.
12. Geijsen N, Horoschak M, Kim K, Gribnau J, Eggan K, Daley GQ: **Derivation of embryonic germ cells and male gametes from embryonic stem cells.** *Nature* 2004, **427:**148-154.
13. Johnson J, Canning J, Kaneko T, Pru JK, Tilly JL: **Germline stem cells and follicular renewal in the postnatal mammalian ovary.** *Nature* 2004, **428:**145-150.
14. Duke KL: **Ovogenetic activity of the fetal-type in the ovary of the adult slow loris, Nycticebus coucang.** *Folia Primatol (Basel)* 1967, **7:**150-154.
15. Ioannou JM: **Oogenesis in adult prosimians.** *J Embryol Exp Morphol* 1968, **17:**139-145.
16. Butler H, Juma MB: **Oogenesis in an adult prosimian.** *Nature* 1970, **226:**552-553.
17. David GF, Anand Kumar TC, Baker TG: **Uptake of tritiated thymidine by primordial germinal cells in the ovaries of the adult slender loris.** *J Reprod Fertil* 1974, **41:**447-451.
18. Telfer EE: **Germline stem cells in the postnatal mammalian ovary: A phenomenon of prosimian primates and mice?** *Reprod Biol Endocrinol* 2004, **2:** 24.
19. Motta PM, Makabe S: **Germ cells in the ovarian surface during fetal development in humans. A three-dimensional microanatomical study by scanning and transmission electron microscopy.** *J Submicrosc Cytol* 1986, **18:**271-290.
20. Simkins CS: **Development of the human ovary from birth to sexual maturity.** *J Anat* 1932, **51:**465-505.
21. Van Blerkom J, Motta PM: *The Cellular Basis of Mammalian Reproduction. Baltimore-Munich: Urban & Schwarzenberg* 1979.
22. Motta PM, Van Blerkom J, Makabe S: **Changes in the surface morphology of ovarian 'germinal' epithelium during the reproductive cycle and in some pathological conditions.** *J Submicrosc Cytol* 1980, **12:**407-425.
23. Makabe S, Iwaki A, Hafez ESE, Motta PM: **Physiomorphology of fertile and infertile human ovaries.** In *Biology of the Ovary* Edited by: Motta PM, Hafez ESE. The Hague: Martinus Nijhoff Publishers; 1980:279-290.
24. Gillett WR: **Artefactual loss of human ovarian surface epithelium: potential clinical significance.** *Reprod Fertil Dev* 1991, **3:**93-98.
25. Mossman HW, Duke KL: **Some comparative aspects of the mammalian ovary.** In *Handbook of Physiology, Sect. 7: Endocrinology* Edited by: Greep RO. Washington: Am. Physiol. Soc; 1973:389-402.
26. Dyck HG, Hamilton TC, Godwin AK, Lynch HT, Maines-Bandiera S, Auersperg N: **Autonomy of the epithelial phenotype in human ovarian surface epithelium: changes with neoplastic progression and with a family history of ovarian cancer.** *Int J Cancer* 1996, **69:**429-436.
27. Auersperg N, Pan J, Grove BD, Peterson T, Fisher J, Maines-Bandiera S, Somasiri A, Roskelley CD: **E-cadherin induces mesenchymal-to-epithelial transition in human ovarian surface epithelium.** *Proc Natl Acad Sci U S A* 1999, **96:**6249-6254.
28. Auersperg N, Wong AS, Choi KC, Kang SK, Leung PC: **Ovarian surface epithelium: biology, endocrinology, and pathology.** *Endocr Rev* 2001, **22:**255-288.
29. Choi KC, Auersperg N, Leung PC: **Mitogen-activated protein kinases in normal and (pre)neoplastic ovarian surface epithelium.** *Reprod Biol Endocrinol* 2003, **1:**71.
30. Treisman R: **Regulation of transcription by MAP kinase cascades.** *Curr Opin Cell Biol* 1996, **8:**205-215.
31. Bukovsky A, Caudle MR, Keenan JA: **Regulation of ovarian function by immune system components: the tissue control system (TCS).** In *Microscopy of Reproduction and Development: A Dynamic Approach* Edited by: Motta PM. Roma: Antonio Delfino Editore; 1997:79-89.
32. Bukovsky A, Keenan JA, Caudle MR, Wimalasena J, Upadhyaya NB, Van Meter SE: **Immunohistochemical studies of the adult human ovary: possible contribution of immune and epithelial factors to folliculogenesis.** *Am J Reprod Immunol* 1995, **33:**323-340.
33. Richer M, Burch LH, Hirsh AJ, Spychala J, Boucher RC: **Ecto 5'-nucleotidase and nonspecific alkaline phosphatase. Two AMP-hydrolyzing ectoenzymes with distinct roles in human airways.** *J Biol Chem* 2003, **278:**13468-13479.

34. Ziomek CA, Lepire ML, Torres I: **A highly fluorescent simultaneous azo dye technique for demonstration of nonspecific alkaline phosphatase activity.** *J Histochem Cytochem* 1990, **38:**437-442.
35. Quinones JA, van Bogaert LJ: **Nonspecific alkaline phosphatase activity in normal and diseased human breast.** *Acta Histochem* 1979, **64:**106-112.
36. Page-Roberts BA: **Changes in nonspecific alkaline phosphatase activity in the rat urinary bladder wall in response to experimental filling.** *Invest Urol* 1972, **9:**385-389.
37. Pan J, Auersperg N: **Spatiotemporal changes in cytokeratin expression in the neonatal rat ovary.** *Biochem Cell Biol* 1998, **76:**27-35.
38. Skinner SM, Dunbar BS: **Localization of a carbohydrate antigen associated with growing oocytes and ovarian surface epithelium.** *J Histochem Cytochem* 1992, **40:**1031-1036.
39. Skinner SM, Lee VH, Kieback DG, Jones LA, Kaplan AL, Dunbar BS: **Identification of a meiotically expressed carbohydrate antigen in ovarian carcinoma: I. Immunohistochemical localization.** *Anticancer Res* 1997, **17:**901-906.
40. Skinner SM, Kieback DG, Chunn J, Jones LA, Metzger DA, Malinak LR, Dunbar BS: **Identification of a meiotically expressed carbohydrate antigen in ovarian carcinoma: II. Association with proteins in tumors and peritoneal fluid.** *Anticancer Res* 1997, **17:**907-911.
41. Dunbar BS, Timmons TM, Skinner SM, Prasad SV: **Molecular analysis of a carbohydrate antigen involved in the structure and function of zona pellucida glycoproteins.** *Biol Reprod* 2001, **65:**951-960.
42. Wartenberg H: **Germ cell migration induced and guided by somatic cell interaction.** *Bibl Anat* 1983, **24:**67-76.
43. Zamboni L: **Ultrastructure of mammalian oocytes and ova.** *Biol Reprod Suppl* 1970, **2:**44-63.
44. Carlson JL, Bakst MR, Ottinger MA: **Developmental stages of primary oocytes in turkeys.** *Poult Sci* 1996, **75:**1569-1578.
45. Motta PM, Nottola SA, Makabe S, Heyn R: **Mitochondrial morphology in human fetal and adult female germ cells.** *Hum Reprod* 2000, **15 Suppl 2:**129-147.
46. Cox RT, Spradling AC: **A Balbiani body and the fusome mediate mitochondrial inheritance during Drosophila oogenesis.** *Development* 2003, **130:**1579-1590.
47. Santini D, Ceccarelli C, Mazzoleni G, Pasquinelli G, Jasonni VM, Martinelli GN: **Demonstration of cytokeratin intermediate filaments in oocytes of the developing and adult human ovary.** *Histochemistry* 1993, **99:**311-319.
48. Motta PM, Makabe S, Naguro T, Correr S: **Oocyte follicle cells association during development of human ovarian follicle. A study by high resolution scanning and transmission electron microscopy.** *Arch Histol Cytol* 1994, **57:**369-394.
49. Pepling ME, Spradling AC: **Mouse ovarian germ cell cysts undergo programmed breakdown to form primordial follicles.** *Dev Biol* 2001, **234:**339-351.
50. Pepling ME, Spradling AC: **Female mouse germ cells form synchronously dividing cysts.** *Development* 1998, **125:**3323-3328.
51. Ingram DL: **Atresia.** In *The Ovary* Edited by: Zuckerman S. London: Academic Press; 1962:247-273.
52. Erickson BH: **Development and senescence of the postnatal bovine ovary.** *J Anim Sci* 1966, **25:**800-805.
53. Block E: **Quantitative morphological investigations of the follicular system in women. Variations at different ages.** *Acta Anat (Basel)* 1952, **14:**108-123.
54. Gougeon A, Echochard R, Thalabard JC: **Age-related changes of the population of human ovarian follicles: increase in the disappearance rate of non-growing and early- growing follicles in aging women.** *Biol Reprod* 1994, **50:**653-663.
55. Bukovsky A, Presl J: **Origin of "definitive" oocytes in the mammal ovary.** *Cesk Gynekol* 1977, **42:**285-294.
56. Bukovsky A, Caudle MR, Keenan JA, Elder RF: **Immune system involvement in the regulation of ovarian function: an immunohistochemical study of the developing and adult human ovary and ovarian cancer.** *Microsc Res Tech* 2004 in press.
57. Bukovsky A, Cekanova M, Caudle MR, Wimalasena J, Foster JS, Henley DC, Elder RF: **Expression and localization of estrogen receptor-alpha protein in normal and abnormal term placentae and stimulation of trophoblast differentiation by estradiol.** *Reprod Biol Endocrinol* 2003, **1:**13.
58. Sehgal S, Gupta SK, Bhatnagar P: **Long-term effects of immunization with porcine zona pellucida on rabbit ovaries.** *Pathology* 1989, **21:**105-110.
59. Miller CC, Fayrer-Hosken RA, Timmons TM, Lee VH, Caudle AB, Dunbar BS: **Characterization of equine zona pellucida glycoproteins by polyacrylamide gel electrophoresis and immunological techniques.** *J Reprod Fertil* 1992, **96:**815-825.
60. Horejsi V, Hilgert I, Kristofova H, Bazil V, Bukovsky A, Kulhankova J: **Monoclonal antibodies against human leucocyte antigens. I. Antibodies against beta-2-microglobulin, immunoglobulin kappa light chains, HLA-DR-like antigens, T8 antigen, T1 antigen, a monocyte antigen, and a pan-leucocyte antigen.** *Folia Biol (Praha)* 1986, **32:**12-25.
61. McKenzie JL, Fabre JW: **Human Thy-1: unusual localization and possible functional significance in lymphoid tissues.** *J Immunol* 1981, **126:**843-850.
62. Sternberger LA, Joseph SA: **The unlabelled antibody method. Contrasting color staining of paired hormones without antibody removal.** *J Histochem Cytochem* 1979, **27:**1424-1429.
63. Block E: **Quantitative morphological investigations of the follicular system in women. Methods of quantitative determinations.** *Acta Anat (Basel)* 1951, **12:**267-285.
64. Block E: **A quantitative morphological investigation of the follicular system in newborn female infants.** *Acta Anat (Basel)* 1953, **17:**201-206.
65. Prindull G, Zipori D: **Environmental guidance of normal and tumor cell plasticity: epithelial mesenchymal transitions as a paradigm.** *Blood* 2004, **103:**2892-9.
66. Kloc M, Bilinski S, Dougherty MT, Brey EM, Etkin LD: **Formation, architecture and polarity of female germline cyst in Xenopus.** *Dev Biol* 2004, **266:**43-61.
67. Klein J: *Immunology: The Science of Self-Nonself Discrimination* New York: John Wiley and Sons, Inc; 1982.
68. Wang F, Riley JC, Behrman HR: **Immunosuppressive levels of glucocorticoid block extra uterine luteolysins in the rat.** *Biol Reprod* 1993, **49:**66-73.
69. Allen E: **Ovogenesis during sexual maturity.** *Am J Anat* 1923, **31:**439-481.
70. Evans HM, Swezy O: **Ovogenesis and the normal follicular cycle in adult mammalia.** *Mem Univ Calif* 1931, **9:**119-224.
71. Jiang Y, Vaessen B, Lenvik T, Blackstad M, Reyes M, Verfaillie CM: **Multipotent progenitor cells can be isolated from postnatal murine bone marrow, muscle, and brain.** *Exp Hematol* 2002, **30:**896-904.
72. Reyes M, Dudek A, Jahagirdar B, Koodie L, Marker PH, Verfaillie CM: **Origin of endothelial progenitors in human postnatal bone marrow.** *J Clin Invest* 2002, **109:**337-346.
73. Van Damme A, Vanden DriesscheT, Collen D, Chuah MK: **Bone marrow stromal cells as targets for gene therapy.** *Curr Gene Ther* 2002, **2:**195-209.
74. Keene CD, Ortiz-Gonzalez XR, Jiang Y, Largaespada DA, Verfaillie CM, Low WC: **Neural differentiation and incorporation of bone marrow-derived multipotent adult progenitor cells after single cell transplantation into blastocyst stage mouse embryos.** *Cell Transplant* 2003, **12:**201-213.
75. Muguruma Y, Reyes M, Nakamura Y, Sato T, Matsuzawa H, Miyatake H, Akatsuka A, Itoh J, Yahata T, Ando K, Kato S, Hotta T: **In vivo and in vitro differentiation of myocytes from human bone marrow-derived multipotent progenitor cells.** *Exp Hematol* 2003, **31:**1323-1330.
76. Gohda E, Nakamura S, Yamamoto I, Minowada J: **Hepatocyte growth factor – pleiotropic cytokine produced by human leukemia cells.** *Leuk Lymphoma* 1995, **19:**197-205.
77. Rubin JS, Bottaro DP, Chedid M, Miki T, Ron D, Cunha GR, Finch PW: **Keratinocyte growth factor as a cytokine that mediates mesenchymal-epithelial interaction.** *EXS* 1995, **74:**191-214.
78. Zarnegar R: **Regulation of HGF and HGFR gene expression.** *EXS* 1995, **74:**33-49.
79. Eshel I, Savion N, Shoham J: **Analysis of thymic stromal cell subpopulations grown in vitro on extracellular matrix in defined medium. II. Cytokine activities in murine thymic epithelial and mesenchymal cell culture supernatants.** *J Immunol* 1990, **144:**1563-1570.
80. Okada H, Danoff TM, Kalluri R, Neilson EG: **Early role of Fsp1 in epithelial-mesenchymal transformation.** *Am J Physiol* 1997, **273:**F563-F574.

81. Sakata M, Shiba H, Komatsuzawa H, Fujita T, Ohta K, Sugai M, Suginaka H, Kurihara H: **Expression of osteoprotegerin (osteoclastogenesis inhibitory factor) in cultures of human dental mesenchymal cells and epithelial cells.** *J Bone Miner Res* 1999, **14:**1486-1492.
82. Kedinger M, Duluc I, Fritsch C, Lorentz O, Plateroti M, Freund JN: **Intestinal epithelial-mesenchymal cell interactions.** *Ann N Y Acad Sci* 1998, **859:**1-17.
83. Bukovsky A, Caudle MR, Keenan JA, Upadhyaya NB, Van Meter SE, Wimalasena J, Elder RF: **Association of mesenchymal cells and immunoglobulins with differentiating epithelial cells.** *BMC Dev Biol* 2001, **1:**11.
84. Motta PM, Makabe S: **Development of the ovarian surface and associated germ cells in the human fetus.** *Cell Tissue Res* 1982, **226:**493-510.
85. Motta PM, Makabe S: **Elimination of germ cells during differentiation of the human ovary: an electron microscopic study.** *Eur J Obstet Gynecol Reprod Biol* 1986, **22:**271-286.
86. Cowley S, Paterson H, Kemp P, Marshall CJ: **Activation of MAP kinase kinase is necessary and sufficient for PC12 differentiation and for transformation of NIH 3T3 cells.** *Cell* 1994, **77:**841-852.
87. Gotoh Y, Matsuda S, Takenaka K, Hattori S, Iwamatsu A, Ishikawa M, Kosako H, Nishida E: **Characterization of recombinant Xenopus MAP kinase kinases mutated at potential phosphorylation sites.** *Oncogene* 1994, **9:**1891-1898.
88. Williams AF, Barclay AN: **The immunoglobulin superfamily-domains for cell surface recognition.** *Annu Rev Immunol* 1988, **6:**381-405.
89. Bukovsky A, Caudle MR, Keenan JA, Wimalasena J, Foster JS, Van Meter SE: **Quantitative evaluation of the cell cycle-related retinoblastoma protein and localization of Thy-1 differentiation protein and macrophages during follicular development and atresia, and in human corpora lutea.** *Biol Reprod* 1995, **52:**776-792.
90. Bukovsky A, Michael SD, Presl J: **Cell-mediated and neural control of morphostasis.** *Meet Hypotheses* 1991, **36:**261-268.
91. Miller RA: **Aging and immune function.** *Int Rev Cytol* 1991, **124:**187-215.
92. Weksler ME: **Immune senescence.** *Ann Neurol* 1994, **35(Suppl):**S35-S37.
93. Sunderkotter C, Kalden H, Luger TA: **Aging and the skin immune system.** *Arch Dermatol* 1997, **133:**1256-1262.
94. Bukovsky A, Caudle MR, Keenan JA, Wimalasena J, Upadhyaya NB, Van Meter SE: **Is corpus luteum regression an immune-mediated event? Localization of immune system components, and luteinizing hormone receptor in human corpora lutea.** *Biol Reprod* 1995, **53:**1373-1384.
95. **Report of the United Nations Scientific Committee on the effects of atomic radiation.** In *General Assembly Official Records: 17th Session, Suppl. No. 16 (A/5216)* New York: United Nations; 1962:12.
96. Sachs ES, Jahoda MG, Niermeijer MF, Galjaard H: **An unexpected high frequency of trisomic fetuses in 229 pregnancies monitored for advanced maternal age.** *Hum Genet* 1977, **36:**43-46.
97. Tsuji K, Nakano R: **Chromosome studies of embryos from induced abortions in pregnant women age 35 and over.** *Obstet Gynecol* 1978, **52:**542-544.
98. Hook EB, Cross PK, Schreinemachers DM: **Chromosomal abnormality rates at amniocentesis and in live-born infants.** *JAMA* 1983, **249:**2034-2038.
99. Eichenlaub-Ritter U: **Parental age-related aneuploidy in human germ cells and offspring: a story of past and present.** *Environ Mol Mutagen* 1996, **28:**211-236.
100. Sakurada K, Ishikawa H, Endo A: **Cytogenetic effects of advanced maternal age and delayed fertilization on first- cleavage mouse embryos.** *Cytogenet Cell Genet* 1996, **72:**46-49.
101. Ginsburg C, Fokstuen S, Schinzel A: **The contribution of uniparental disomy to congenital development defects in children born to mothers at advanced childbearing age.** *Am J Med Genet* 2000, **95:**454-460.
102. Krey L, Liu H, Zhang J, Grifo J: **Fertility and maternal age strategies to improve pregnancy outcome.** *Ann N Y Acad Sci* 2001, **943:**26-33.
103. Gianaroli L, Magli MC, Ferraretti AP, Tabanelli C, Trombetta C, Boudjema E: **The role of preimplantation diagnosis for aneuploidies.** *Reprod Biomed Online* 2002, **4(Suppl 3):**31-36.
104. Munne S: **Preimplantation genetic diagnosis of numerical and structural chromosome abnormalities.** *Reprod Biomed Online* 2002, **4:**183-196.
105. L'Hermine AC, Aboura A, Brisset S, Cuisset L, Castaigne V, Labrune P, Frydman R, Tachdjian G: **Fetal phenotype of Prader-Willi syndrome due to maternal disomy for chromosome 15.** *Prenat Diagn* 2003, **23:**938-943.
106. Munne S: **Preimplantation genetic diagnosis and human implantation-a review.** *Placenta* 2003, **24(Suppl B):**S70-S76.
107. Parker MJ, Budd JL, Draper ES, Young ID: **Trisomy 13 and trisomy 18 in a defined population: epidemiological, genetic and prenatal observations.** *Prenat Diagn* 2003, **23:**856-860.
108. Pehlivan T, Rubio C, Rodrigo L, Remohi J, Pellicer A, Simon C: **Preimplantation genetic diagnosis by fluorescence in situ hybridization: clinical possibilities and pitfalls.** *J Soc Gynecol Investig* 2003, **10:**315-322.
109. Pujol A, Durban M, Benet J, Boiso I, Calafell JM, Egozcue J, Navarro J: **Multiple aneuploidies in the oocytes of balanced translocation carriers: a preimplantation genetic diagnosis study using first polar body.** *Reproduction* 2003, **126:**701-711.
110. Eichenlaub-Ritter U, Vogt E, Yin H, Gosden R: **Spindles, mitochondria and redox potential in ageing oocytes.** *Reprod Biomed Online* 2004, **8:**45-58.
111. Kahraman S, Benkhalifa M, Donmez E, Biricik A, Sertyel S, Findikli N, Berkil H: **The results of aneuploidy screening in 276 couples undergoing assisted reproductive techniques.** *Prenat Diagn* 2004, **24:**307-311.
112. Kotzot D: **Advanced parental age in maternal uniparental disomy (UPD): implications for the mechanism of formation.** *Eur J Hum Genet* 2004, **12:**343-346.